ANTARCTIC CLIMATE & ECOSYSTEMS CRC

climate futures for tasmania

TECHNICAL REPORT

Extreme Tide and Sea-Level Events

McInnes KL, O'Grady JG, Hemer M, Macadam I, Abbs DJ, White CJ, Corney SP, Grose MR, Holz GK, Gaynor SM & Bindoff NL

January 2012

Climate Futures for Tasmania
Extreme Tide and Sea-Level Events Technical Report

ISBN 978-1-921197-10-9

The Manager
Communications
Antarctic Climate & Ecosystems Cooperative Research Centre

Private Bag 80
Hobart Tasmania 7001
Tel: +61 3 6226 7888, Fax: +61 3 6226 2440
Email: climatefutures@acecrc.org.au

Science Reviewers

Dr Ivan Haigh (University of Western Australia), Professor Keith Thompson (Dalhousie University) and
Dr AS Unnikrishnan (National Institute of Oceanography)

The reviewers listed in this report have offered all comments and recommendations in good faith and in an unbiased and professional manner. At no time was the reviewer asked to verify or endorse the project conclusions and recommendations nor was the reviewer privy to the final draft of the report before its release.

The reviewers' role was solely advisory and should not be construed as an endorsement of the project findings by the reviewer or his /her employing organisation. Neither the reviewer nor his/her employing organisation provides any representation or warranty as to the accuracy or suitability of any project findings. Responsibility for all work done in connection with the project remains with the project team.

Photo Credits: Suzie Gaynor (p 2), Miranda Harman (pp Front Cover, 5), John Hunter (p 18), Tessa Jakszewicz (pp 13, 21, 40).

Graphic Design: Suzie Gaynor

Citation

McInnes KL, O'Grady JG, Hemer M, Macadam I, Abbs DJ, White CJ, Corney SP, Grose MR, Holz GK, Gaynor SM & Bindoff NL 2011, *Climate Futures for Tasmania: extreme tide and sea-level events technical report*, Antarctic Climate and Ecosystems Cooperative Research Centre, Hobart, Tasmania.

TECHNICAL REPORT

Climate Futures for Tasmania: extreme tide and sea-level events

McInnes KL, O'Grady JG, Hemer M, Macadam I, Abbs DJ, White CJ, Corney SP,

Grose MR, Holz GK, Gaynor SM & Bindoff NL

January 2012

Foreword

The Climate Futures for Tasmania research project is the key source of information for the Tasmanian Government's Climate Change Strategy. A number of the outputs from the project will have long-term strategic implications for emergency management and local government planning in Tasmania.

The outputs from the Extreme Tide and Sea-Level Events Technical Report will be helpful in supporting evidence-based policy and decision-making for the management of Tasmanian coasts. This scientific report uses the most comprehensive and current scientific methods available for the evaluation of sea-level extremes and the projection of their changes in response to rising greenhouse gases. It is a pleasure to see how these new projections of extreme sea levels have already been used by policy makers with other research products from the Climate Futures for Tasmania project. An example of this is the development of coastal inundation models that estimate the likelihood of inundation by extreme events in selected vulnerable regions around Tasmania. This work undertaken by the Blue Wren Group and the Antarctic Climate & Ecosystems Cooperative Research Centre (ACE) combined both the LiDAR (Light Detection and Ranging) Dataset and the extreme sea-level results - the subject of this report.

This unique and leading research will enable the Tasmanian Government to work in partnership with stakeholders to assist communities around the State to adapt to climate change and minimise the adverse effects of extreme sea levels. The extreme weather events around the country in 2011 highlighted the importance of this project. No longer can we assume that we are immune from the damaging impacts of extreme weather events. Tasmanian communities can prepare for these events by obtaining a high-level understanding of the impacts of climate change.

This report, led by Dr Kathleen McInnes and her team from CSIRO and ACE, has provided the underlying science. The outputs from this report are strong and robust and the research can be directly applied in decision-making.

The report has passed the rigours of an external scientific review. I appreciate the efforts of the respected scientists who provided their expertise and time to confirm the research outcomes. In particular, I thank Professor Keith Thompson (Dalhousie University, Canada), Dr Ivan Haigh (University of Western Australia) and Dr AS Unnikrishnan (National Institute of Oceanography, India).

Tasmanian communities will benefit from this Extreme Tide and Sea-Level Events report from the Climate Futures for Tasmania research project. All those involved in the project are to be congratulated for their valuable contribution to emergency management in Tasmania.

Prof Nathan Bindoff, ACE CRC

Executive Summary

Rising sea levels are a consequence of a warming climate and will be felt most acutely during extreme sea-level events brought about by the combination of storm surges and high tides which may cause coastal inundation and erosion.

The purpose of this study has been to investigate the causes of extreme sea levels and evaluate their return periods for late 20th century conditions along the Tasmanian coast. These data provide a basis for estimating the impact of rising sea levels on the extreme sea-level return periods and of estimating land at risk from inundation due to projected future sea levels.

Storm surges on the southeast coast of Tasmania are typically less than a metre in height and are mainly caused when cold fronts cross the region.

Tide-gauge records show that storm surges on the southeast coast of Tasmania attain maximum heights of typically less than a metre and the weather systems most commonly responsible for generating elevated sea levels at these locations are the west to east moving cold frontal systems associated with low pressure centres situated to the south of Tasmania. While such systems were also the cause of elevated sea levels on the Tasmanian north coast, the largest storm-surge events there occurred when a low pressure centre was situated to the west of Tasmania or Bass Strait and brought strong northerly winds to this coastline.

The high correlation between storm surges on the Tasmanian coast with those on the mainland coast means that information about Tasmanian storm surges can be obtained by combining Tasmanian tide-gauge information with that from the mainland coast.

The high correlation between storm surges on the Tasmanian and Victorian coasts meant that a more efficient modelling approach, previously applied to the Victorian coast, could be used to evaluate storm-surge return levels for the Tasmanian coast. In this, a population of extreme sea-level generating weather events was identified from a limited number of long tide-gauge records and each of the events modelled with a hydrodynamic model forced with archived wind and pressure patterns. The peak residual sea levels from each event were then statistically analysed to obtain event probabilities. This modelling indicated that the highest storm-surges occurred on the southeastern coastline of Tasmania and storm surges were lowest on the northern Tasmanian coast.

New estimates of one-in-100-year sea levels for Tasmania have been developed.

Tide prediction models are used to generate probability distributions of tide height. The tidal range was largest on the Tasmanian north coast and smallest on the southwest coast. Tide height probability distributions were developed and combined with storm surges to yield return periods of storm tide (the total sea level arising from the combination of a storm surge and tide). The one-in-100-year sea levels for Hobart, Georgetown, Burnie and Spring Bay were estimated to be 1.29, 2.00, 1.92 and 0.99 m relative to Australian Height Datum (AHD) respectively.

Projected future changes in wind speed were found to have a negligible effect on future storm surges.

Changes in wind speed are not projected to significantly affect storm surge. The effect on storm surges of wind speed changes was investigated by adjusting the winds in each event by the wind changes in the 2080 to 2099 climate relative to the 1980 to 1999 climate. The changes were found to vary from no change to negligible reduction in storm tide height around the Tasmanian coast. Further investigation is needed to understand the role of wind changes on the Tasmanian coast results presented here, but are beyond the scope of the current project.

By 2100 projected sea-level rise will mean that a 100-year event based on late 20th century conditions will occur between 15-100 times more often.

By 2030 a 100-year event based on late 20th century conditions will occur around twice to 10 times more often (i.e. about once every 10 to 50 years) if sea-level rise follows the upper end of the IPCC (2007) projected range. By 2090, a 100-year event based on late 20th century conditions will occur as frequently as once every five years and up to several times a year if the high-end projections for sea-level rise eventuate.

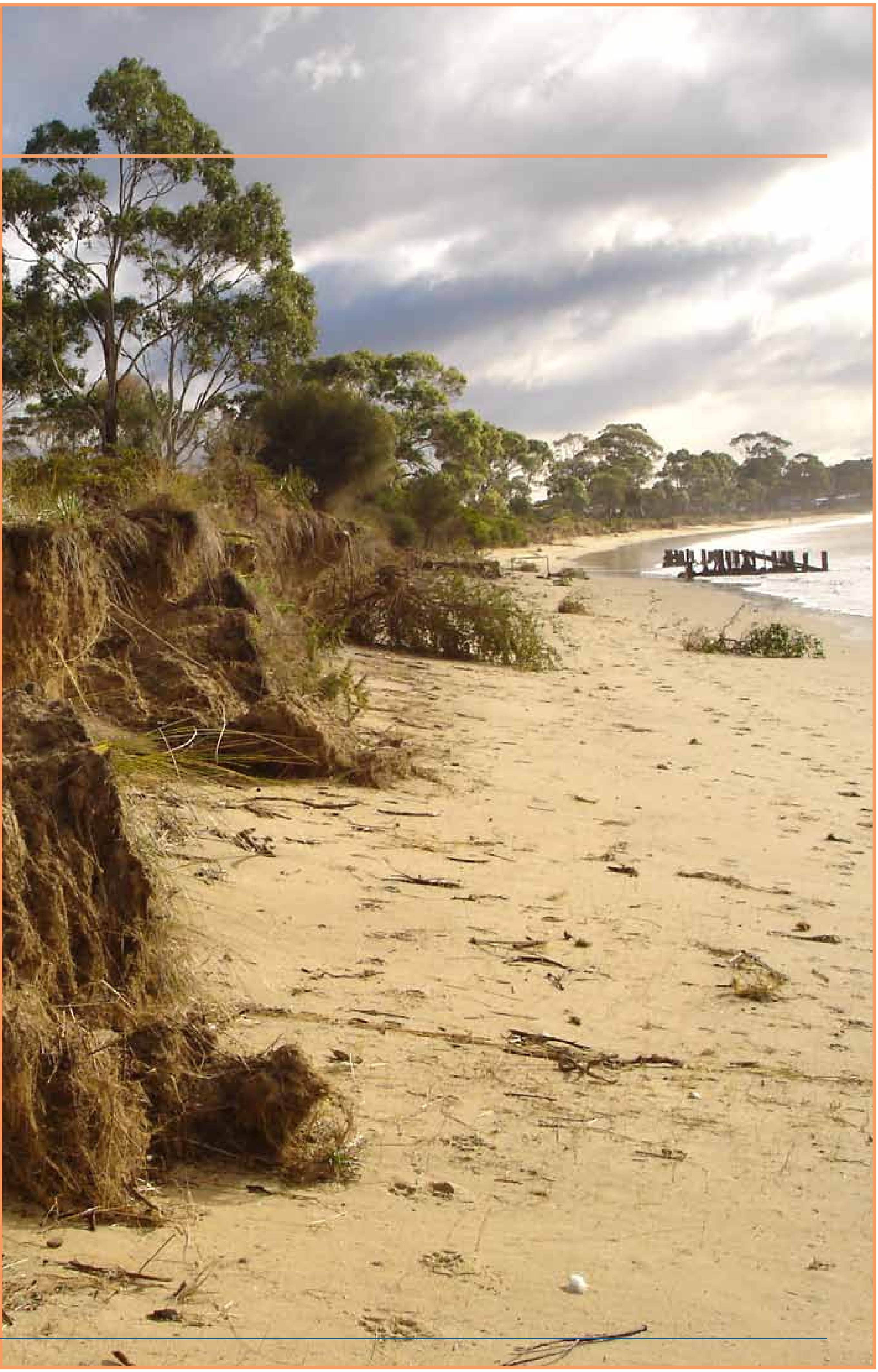

FREQUENTLY USED ABBREVIATIONS

Average Recurrence Interval	ARI
Digital Elevation Model	DEM
Generalised Extreme Value	GEV
Global Climate Model	GCM
Intergovernmental Panel on Climate Change	IPCC
Joint Probability Method	JPM
National Centers for Environmental Prediction	NCEP
Root Mean Square	RMS

Table of Contents

1 Introduction

Sea levels have been rising at an increasing rate since the early 1800s. The average rate of sea-level rise over the 20th century of 1.7 ± 0.5 mm yr^{-1} (Bindoff et al 2007) has led to a change in the frequency of extreme events. Over the period 1993-2006, mean sea-level trends based on both reconstructed sea-level (Church and White 2006) and satellite altimetry have increased to 3.3 ± 0.4 mm yr^{-1}. This rate of increase is consistent with the upper envelope of the Intergovernmental Panel on Climate Change (IPCC) sea-level projections (Rahmstorf et al. 2007), which is associated with a globally averaged sea-level increase of 0.82 m by 2100 (Hunter 2010). The IPCC concluded that extreme high water levels associated with storm surges have undergone a likely increasing trend across the globe during the 20th century (Bindoff et al 2007). Recent studies have found that these trends appear to be driven largely by trends in mean sea level rather than changes in storminess (Menendez and Woodworth 2010; Woodworth et al 2011). These observed and projected changes in sea level pose threats for coastal settlements that have developed during the period of relatively stable sea levels of the previous two millennia (Jansen et al 2007).

Sea-level rise will be felt most acutely during severe storm events when strong winds and lower than normal atmospheric pressure drive storm surges and high waves. Impacts of these events will be greatest when they occur at high tide. Such events can cause inundation of low lying coastal terrain, severe erosion and wave overtopping.

In recent years, concern over the potential adverse impacts of rising sea levels has seen a number of programs and initiatives undertaken by various levels of government to develop information about future coastal vulnerability to climate change. In Tasmania, the Department of Primary Industries, Parks, Water and Environment (DPIPWE) commissioned a 'first pass' mapping of Tasmanian shorelines vulnerable to storm-surge flooding and erosion of sandy shorelines (Sharples, 2006). The Sharples study developed a coastal geomorphic line map in a Geographic Information System framework called 'the Smartline'. Each line segment of the Smartline contained information on a range of shoreline characteristics that facilitated an assessment of coastal vulnerability due to erosion. To support the assessment of risk to communities from coastal inundation the Climate Futures for Tasmania project also supported the acquisition of airborne LiDAR surveys along four selected coastal regions of Tasmania including extensive coastal regions around Storm Bay and D'Entrecasteaux Channel, the Tamar Estuary and North West Coast, Great Oyster Bay including Swansea and Coles Bay and Binnalong Bay including St Helens on the east coast. These data have subsequently been used in combination with storm tide data developed in this project to evaluate vulnerable coastal land for the Tasmania Planning Commission (Mount et al 2010).

This report describes the development of spatial maps of extreme sea level associated with particular recurrence intervals along the Tasmanian coast under climate conditions of the late 20th century using the dynamical modelling of storm surge and a statistical combination of surge and tidal information as described in McInnes et al (2009a, b, c). Some aspects of the storm-surge responses on the northern side of the Bass Strait are also considered since they are important to storm surges around Tasmania. These maps provide a basis for the investigation of the possible impacts of future climate change due to sea-level rise and changes in weather conditions and will provide information for subsequent coastal assessments around Tasmania.

The remainder of this report is structured as follows. The following section describes the nature of extreme sea levels around Tasmania and the weather conditions most commonly responsible for elevated sea levels. Section 3 describes the modelling approach used in this study and Section 4 discusses future climate scenarios. Modelling results are discussed in section 5 and conclusions are summarised in Section 6.

About the project

Climate Futures for Tasmania is the Tasmanian Government's most important source of climate change data at a local scale. It is a key part of Tasmania's climate change strategy as stated in the Tasmanian Framework for Action on Climate Change and is supported by the Commonwealth Environment Research Facilities as a significant project.

The project used a group of global climate models to simulate the Tasmanian climate. The project is unique in Australia: it was designed from conception to understand and integrate the impacts of climate change on Tasmania's weather, water catchments, agriculture and climate extremes, including aspects of sea level, floods and wind damage. In addition, through complementary research projects supported by the project, new assessments were made of the impacts of climate change on coastal processes, biosecurity and energy production, and the development of tools to deliver climate change information to infrastructure asset managers and local government.

As a consequence of this wide scope, Climate Futures for Tasmania is an interdisciplinary and multi institutional collaboration of twelve core participating partners (both state and national organisations). The project was driven by the information requirements of end users and local communities.

The Climate Futures for Tasmania project complements climate analysis and projections done at the continental scale for the Fourth Assessment Report from the Intergovernmental Panel on Climate Change, at the national scale in the Climate Change in Australia Report and data tool, as well as work done in the south-east Australia region in the South Eastern Australia Climate Initiative. The work also complements projections done specifically on water availability and irrigation in Tasmania by the Tasmania Sustainable Yields Project.

2 Background

Coastal sea levels vary on different timescales due to different physical forcing. Astronomical tides cause sea-level variations on a range of timescales ranging from sub-daily (high and low tides), through fortnightly (spring and neap tides) to annual and longer timescales. Low pressure and strong winds associated with severe weather events can cause fluctuations in coastal sea levels which are commonly called storm surges. Associated with storm surges are wind driven waves which can also contribute to elevated sea levels through wave setup. These various contributions are illustrated in Figure 1. Variations in mean sea level also occur on seasonal and inter-annual time scales, the most significant contribution to inter-annual variations in sea levels around Australia being due to the El Niño Southern Oscillation (e.g. Church et al 2006). Superimposed on these variations are the long term increases in sea level due to global warming (Church and White, 2006). The focus of this study is the contribution of storm surges and astronomical tides to extreme sea levels which are referred to as storm tides. Although wave breaking can further elevate sea levels through wave setup and wave runup, these processes are not considered in the present study. This section discusses the meteorological contributions to sea levels, which are identified in tide-gauge records after the removal of the astronomical tides. These contributions are referred to in this report as non-tidal residuals or in more extreme cases, storm surges.

Sea-level extremes may also be affected by nonlocal coastal variations hundreds to thousands of kilometres away. In Tasmania, storm surges are influenced by those variations occurring in Bass Strait and the Victorian coast. Consequently, consideration of the occurrence of extremes around Tasmania must also take into account the effects from further afield. This is particularly important for testing and validating the storm-surge simulations and the methods used here to project the changes in extreme sea level for Tasmania. It is for these reasons that we also consider parts of Victoria as well as Tasmania in this report. A recent investigation of extreme sea levels on the Victorian coast found that the non-tidal component of the measured sea levels was highly correlated between pairs of tide gauges along this coastline (McInnes et al 2009b). This finding led to the development of an efficient approach to modelling extreme sea levels to develop spatially continuous maps of sea level associated with particular return periods. The reason for the high correlation was that the synoptic weather systems responsible for elevated sea levels were mainly frontal systems, which are a large scale feature of the climatology of this region, particularly in the winter months and therefore affect a large stretch of coastline when they occur. This section investigates to what extent this link exists for Tasmanian sea-level extremes and whether the modelling approach applied previously to Victoria can also be applied to Tasmania.

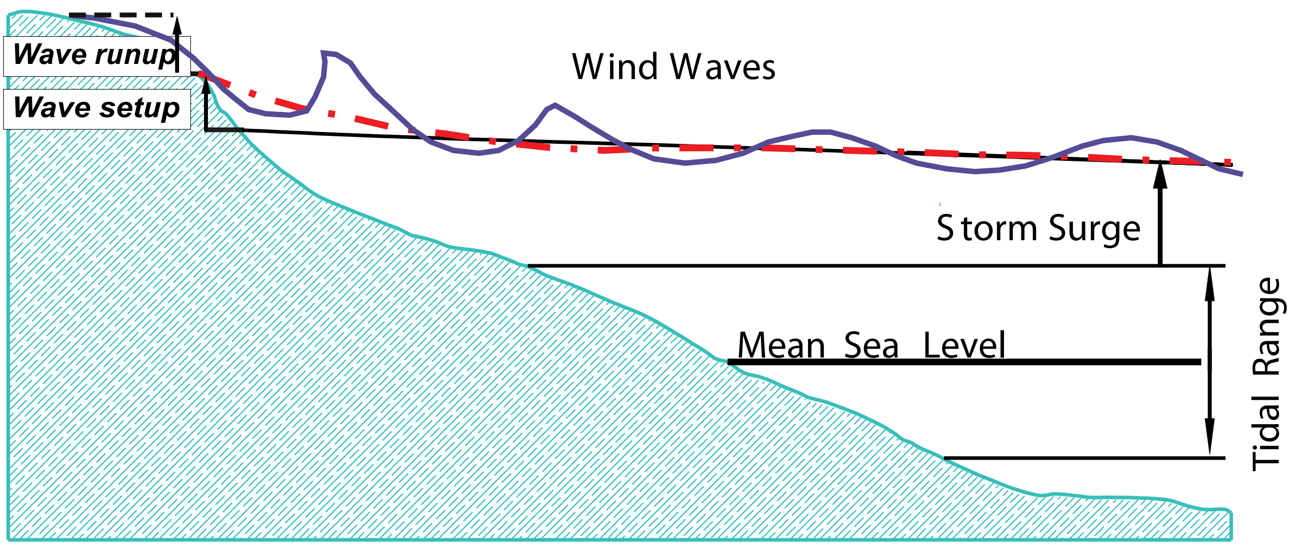

Figure 1: Schematic illustrating the contributions to coastal sea levels. Extreme sea levels comprise some combination of storm surge and astronomical tide which are modelled in this study and are often referred to as a storm tide. Note that a storm tide can comprise a large surge in combination with a small or even negative tide or a moderate surge in combination with a particularly high tide. Sea levels may be further amplified at the coast due to wave breaking processes such as wave setup and runup, however these processes are not considered in this study.

2.1 Relationship between Tasmanian and Victorian Sea-level Extremes

The sea-level records from several tide gauges located along the Victorian and Tasmanian coast were selected to investigate the correlation in sea levels between pairs of gauges. Data was selected from eight tide-gauge records, four from the Victorian coast (Portland, Lorne, Point Lonsdale and Lakes Entrance) and four from the Tasmanian coast (Burnie, George Town, Spring Bay and Hobart) (see Figure 2 for locations). These records were selected from a larger set of available tide gauges because together they spanned the coastlines of Victoria and Tasmania and they also contained more than 10 years of data.

There are two commonly used methods of deriving approximations to the meteorological component of sea-level variability from hourly tide-gauge observations. Numerical filters can be applied to the observed sea levels to remove tidal signals or sea-level residuals can be obtained by subtracting predicted tide heights. The second method however was found to be problematic for the two Victorian stations of Lorne and Stony Point during episodes of elevated sea level (McInnes and Hubbert 2003). During episodes of strong southwesterly winds, when elevated coastal sea levels generally occurred, the residuals obtained by subtracting out the predicted tide contained a pronounced oscillatory signal that was attributed to contamination by the astronomical tide. During strong wind events it appears that a slight phase shift occurs in the tides and this is not removed when tide heights, predicted using tide constants from long tidal records, are subtracted from the measured sea levels. This is illustrated in Figure 3 which compares the method of subtracting the predicted tide and the filtering method, based on Godin (1972), at Portland, Lorne and Stony Point on the Victorian coast and Burnie on the north Tasmanian coast (see Figure 2 for locations).

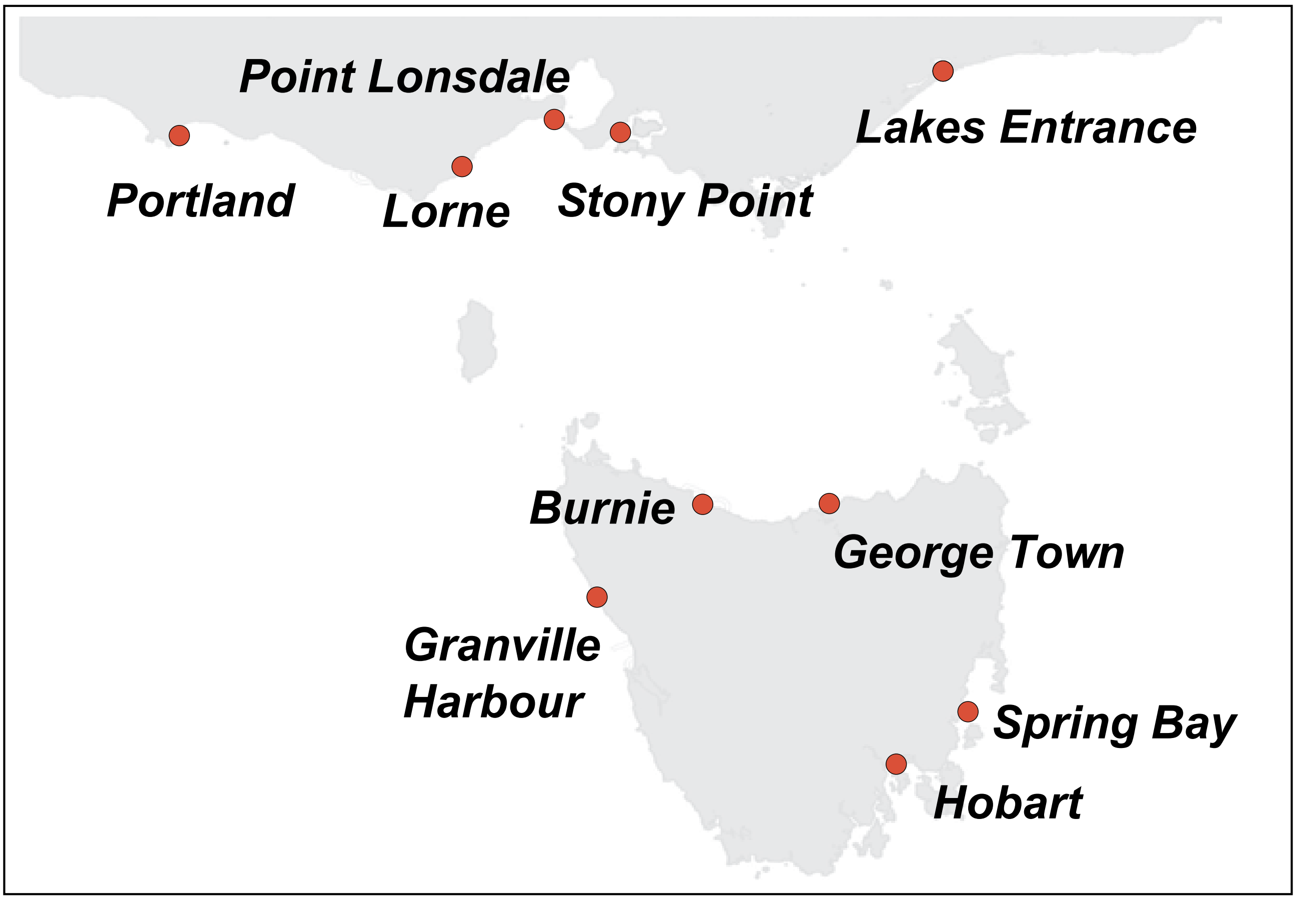

Figure 2: Tide gauge locations referred to in the report.

The two methods produce comparable results at Portland whereas the method of subtracting the predicted tides does not lead to complete removal of the tidal signal at the three central Bass Strait locations of Lorne, Stony Point and Burnie. The issue of the non-linear interaction of tides and surge is discussed more broadly by Horsburgh and Wilson (2007). For the purpose of identifying candidate events for subsequent hydrodynamic modelling, the method of subtracting the predicted tides was not considered suitable and so the filtering method of Godin (1972) was used instead. Although the filtering method may eliminate some of the surge variability resulting in a smoother varying curve than the tide subtraction method, the generation of sea-level residuals is for the purpose of selecting candidate events for later modelling and so will not influence the modelled results in any way.

After applying the method of Godin (1972) to remove sea-level variations due to astronomical tides, a time series containing the maximum daily residual sea levels was then developed. Figure 4 provides an example of the daily maximum residual sea levels for the years 1994 and 2002. In Figure 4a, the particularly long-lived event that occurred in May 1994 and the shorter lived event that occurred in early November 1994 were the subject of more detailed examination in McInnes and Hubbert (2003) and McInnes et al (2009c). The northern Tasmanian locations both show

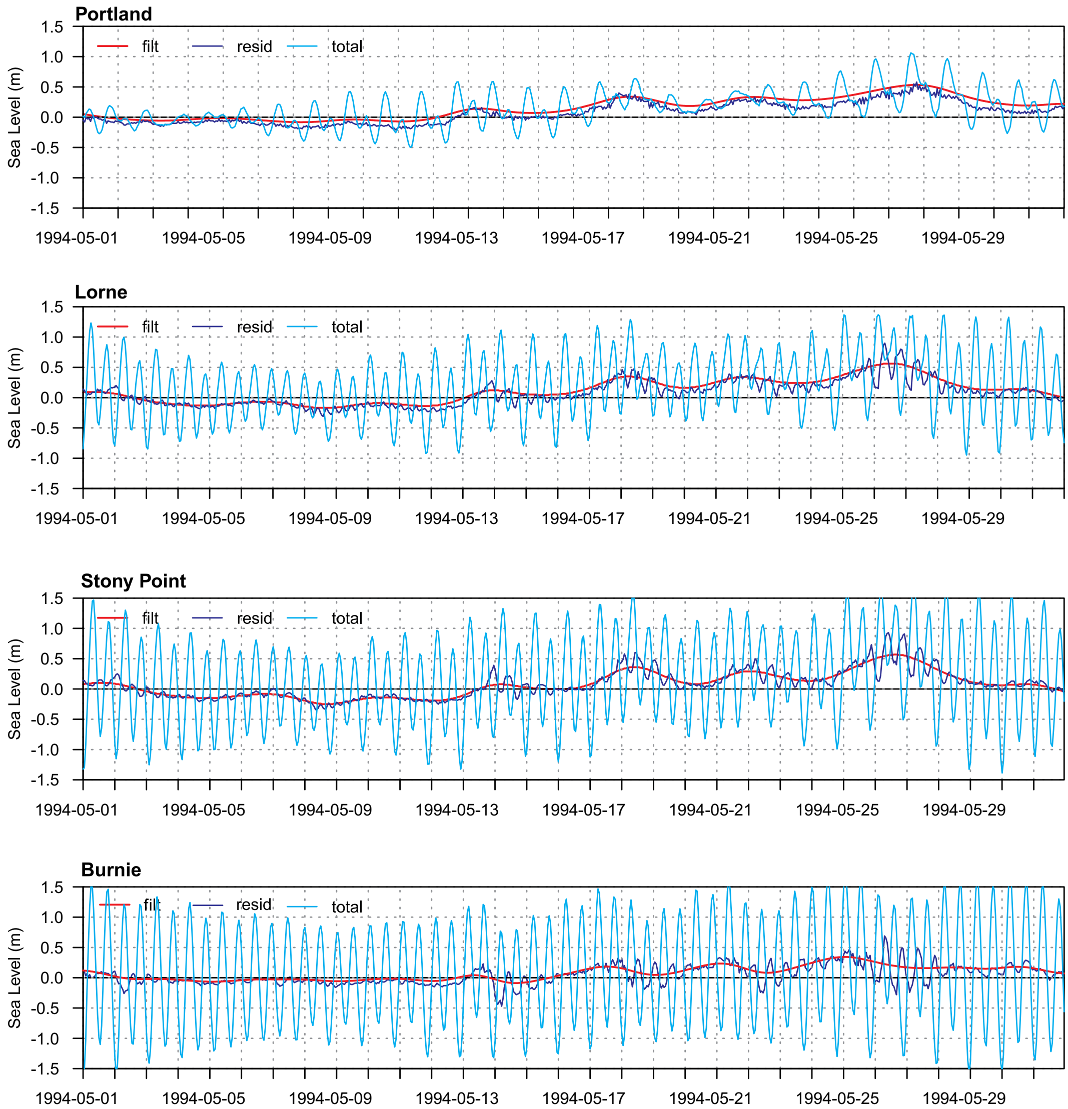

Figure 3: Figures showing total sea level (cyan) and residuals calculated by subtracting the predicted tide (blue) and residuals obtained by filtering out the tidal signal (red). At Portland, the tide subtraction and filtering methods yield similar results, however within Bass Strait at Lorne, Stony Point and Burnie, a residual of the tide remains due to a shift in the phase of the tides which can be seen to occur during episodes when the weather conditions cause higher than normal residual sea levels.

higher than normal residuals during the May event although of smaller magnitude. The November event, while represented by a spike in the non-tidal residuals at Portland, Lorne, Spring Bay and Hobart is extremely weak at Burnie and George Town. Similarly in 2002, there is a signature of a long-lived event in June at all gauges shown whereas a shorter-lived event in early December is not seen at Burnie (Figure 4b).

From the record of daily maximum residuals, correlations between respective pairs of time series were calculated and are presented in Table 1. For the gauges along the Victorian coastline the correlations are high between Portland and Lorne (0.97) but diminish further eastward along the coast, with the daily maximum sea-level residuals between Lakes Entrance and Portland having a correlation of only 0.59.

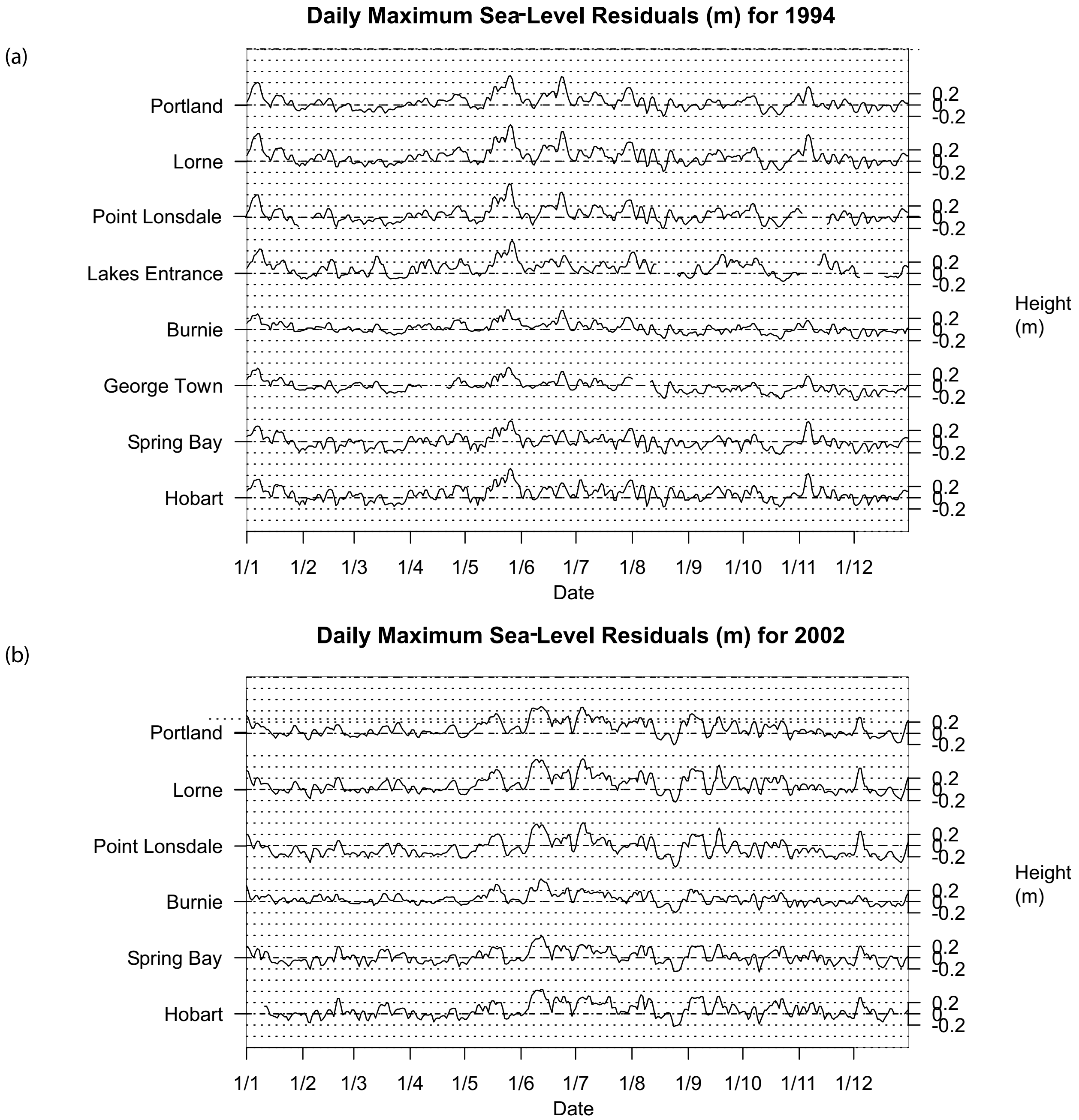

Figure 4: Daily maximum sea-level residuals for (a) 1994 and (b) 2002. Note that Lakes Entrance and George Town sea levels were not available for 2002.

Location	Portland (P)	Lorne (L)	Point Lonsdale (PL)	Lakes Entrance (LE)	Burnie (B)	George-Town (G)	Hobart (H)	Spring Bay (SB)
P	1.00	0.97	0.85	0.56	0.79	0.77	0.80	0.80
L	0.97	1.00	0.97	0.68	0.86	0.87	0.86	0.82
PL	0.85	0.97	1.00	0.63	0.63	0.82	0.85	0.72
LE	0.59	0.68	0.63	1.00	0.41	0.63	0.69	0.62
B	0.79	0.86	0.63	0.41	1.00	0.70	0.64	0.73
G	0.77	0.90	0.82	0.63	0.70	1.00	0.71	0.83
H	0.80	0.87	0.72	0.62	0.64	0.71	1.00	0.98
SB	0.80	0.88	0.85	0.69	0.73	0.83	0.98	1.00

Table 1: Correlation coefficients of daily maximum sea-level residuals between pairs of tide gauge locations. All correlations are significant at the 95% confidence level.

Along the Tasmanian coast, Burnie is most highly correlated with Lorne (0.86) followed by Portland (0.79), both located on the western Victorian coast. George Town is most highly correlated with Lorne (0.90) followed by Spring Bay on the Tasmanian east coast (0.83). Hobart is most highly correlated with Spring Bay (0.98) followed by Lorne (0.87) and is most weakly correlated with Lakes Entrance (0.62), George Town (0.77) and Burnie (0.79).

These data show that sea-level residuals at Hobart and Spring Bay are more highly correlated with those in western and central Victoria than those on the northern Tasmanian coast. Sea-level residuals at Lakes Entrance and northern Tasmania generally exhibit the lowest correlations with each other and other gauges indicating the possible influence of different types of meteorological forcing on sea-level residuals at these locations. It suggests that the approach used in McInnes et al (2004b,c), in which a population of extreme events is selected for modelling on the basis of a small number of representative sea-level records, can be used in the present study with the inclusion of additional tide gauges on the Tasmanian coast.

2.2 Synoptic weather events associated with extreme sea levels

The synoptic weather patterns associated with high sea-level residuals along the Victorian coast were investigated in McInnes et al (2005) and along the northern Tasmanian coast in McInnes et al (2009a) using the Kirchhofer (1973) correlation-based pattern-typing technique described in Yarnal (1993). In this method, fields of gridded numerical data are grouped on the basis of similar spatial structures (that is highs and lows in similar positions) using Pearson product-moment correlations. Relevant results from those studies are summarised here.

On the Victorian coastline, McInnes et al (2005) applied synoptic typing to the mean sea-level pressure patterns on days in which sea-level residuals exceeded 0.4 m at Stony Point and Lakes Entrance, representing the western and eastern coastlines respectively. The threshold was chosen to obtain around 180 events in each record. Because a 38 year record was used for Lakes Entrance whereas only a 12 year record was used for Stony Point, this threshold represented the top 1.5% and 5% of events respectively.

In the western half of the state, high sea-level residuals were found in over 99% of cases to be associated with the weather patterns shown in Figure 5a-c, which represent the eastward travelling cold fronts usually associated with a low pressure system at latitudes south of Tasmania. Winds during these events are generally northwesterly ahead of the front and southwesterly to southerly behind. These weather patterns also accounted for high sea-level residuals at Lakes Entrance in about 70% of cases. The remaining high sea-level days at Lakes Entrance were associated with a low pressure system situated in the south-west of Tasmania (Figure 5d), which brings southerly winds to the eastern Victorian coast.

The synoptic weather conditions from the days on which the highest 80 daily maximum sea-level residuals occurred at Burnie between 1993 and 2003 were investigated in McInnes et al (2009a). Over

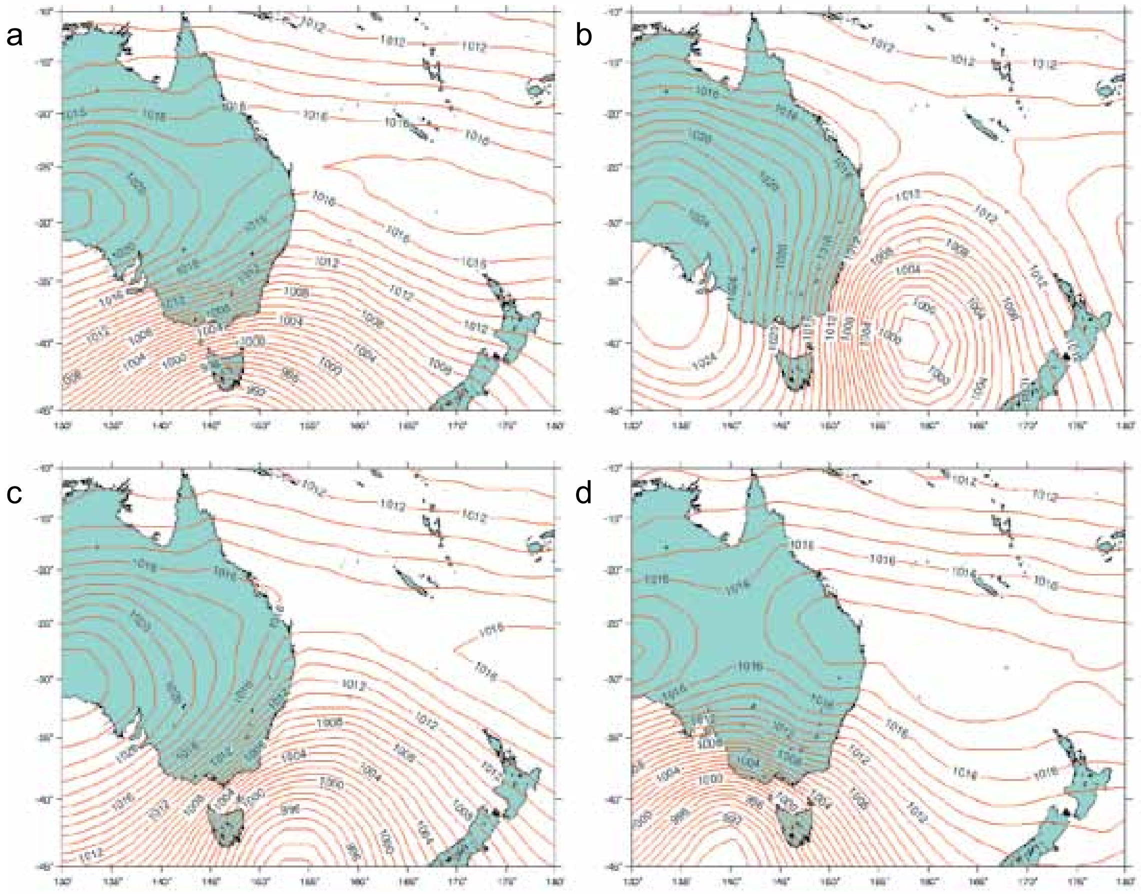

Figure 5: Synoptic weather conditions leading to elevated sea levels on the west coast of Tasmania and the Victorian coast, but lower sea levels on the north and east coast of Tasmania.

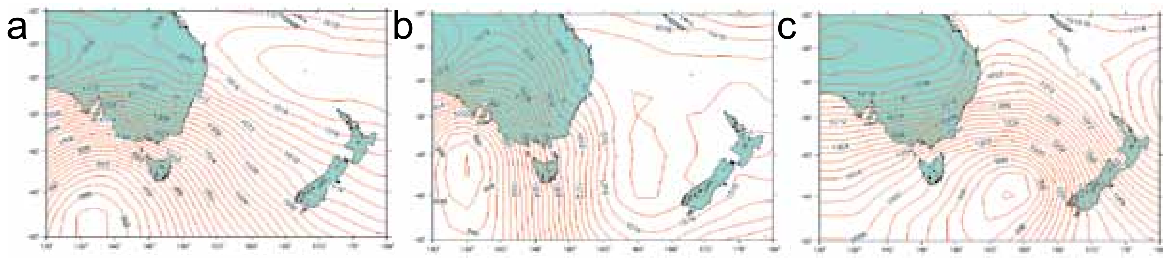

Figure 6: Synoptic weather conditions leading to elevated sea levels on the north coast of Tasmania, but lower or slightly elevated sea levels on west and east coast of Tasmania and Victoria.

85% of the days identified were associated with the patterns shown in Figures 6a and 6b. The first synoptic type accounted for 63% of the patterns on high sea-level days and consisted of a low pressure centre to the southwest of Tasmania bringing northwesterly winds across Bass Strait. This pattern often preceded the arrival of a cold front. The second synoptic pattern accounted for 22% of the high sea-level days and consisted of a depression located at Tasmanian latitudes to the west of Tasmania bringing northwesterly to northeasterly winds to the northern Tasmanian coast. The third pattern (Figure 6c) is typical of the conditions that occur in the latter stages of the passage of a front when it has moved eastwards into the Tasman Sea. This pattern was associated with 14% of high residual days.

2.3 Extreme sea-level event selection

The results in the previous two sections indicate the relationship between sea-level records along the Tasmanian and Victorian coasts. The correlations between Hobart and Spring Bay and the western half of the Victorian coastline are higher than correlations from gauges on the northern Tasmanian coast with other locations. An examination of the synoptic conditions indicates that frontal systems are a major cause of elevated sea levels along both coastlines, although the northern Tasmanian events are more influenced by frontal lows that are situated to the west of Tasmania.

The aim of this study is to use hydrodynamic modelling to generate spatially continuous information about extreme sea-level residuals from which the typical severity and frequency, commonly expressed in return periods or Average Recurrence Intervals (ARIs), can be estimated using extreme-value statistical analysis. This can be accomplished by simulating the residual (non-tidal) sea levels over a continuous interval of time, thereby yielding a record from which extreme residual sea levels can be selected for statistical analysis. However, a computationally more efficient approach is to model only the extreme events. The high coherence of the residual sea levels between tide gauges in this region suggests that the identification of events at a small number of locations will satisfactorily identify the extreme events at all coastal locations around Tasmania and therefore this computationally efficient approach is adopted in this study.

The tide-gauge records from Portland, Point Lonsdale, Lakes Entrance, George Town and Hobart were used to select a population of high residual events for hydrodynamic model simulation. This is because they contained relatively long and complete tide-gauge records that spanned the region of interest and reflected the range of meteorological forcing responsible for extreme sea levels in the region. Gaps in the record were filled using data from other highly correlated tide-gauge records following the procedure described in McInnes et al (2009b). Events were selected on the basis of up and down-crossing of a residual sea-level threshold. The thresholds used for each tide gauge were selected to ensure that at least two events occurred at each location per year for the subsequent statistical analysis. The thresholds for Portland, Point Lonsdale, Lakes Entrance, George Town and Hobart were 0.21, 0.26, 0.22, 0.19 and 0.22 respectively. As expected from the highly-correlated residual sea levels shown in Table 1, there was considerable overlap in the events selected from the different gauges. The overlapping events identified from the different tide gauges were combined into a single set of events spanning the earliest commencement time to the latest completion time. A population of 417 events was selected from approximately 38 years of tide-gauge data from 1964-2002 . This relates to around 11 events per year.

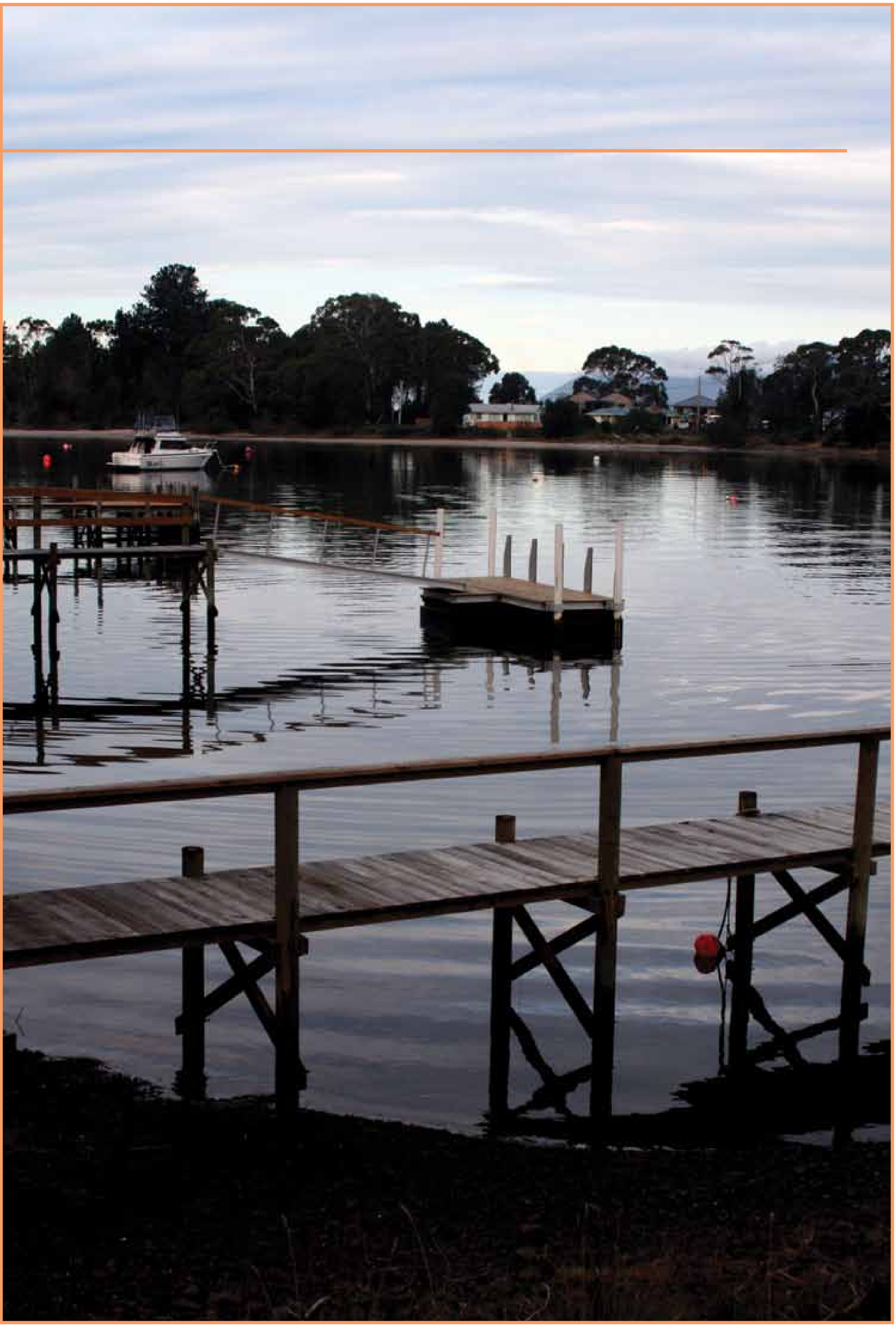

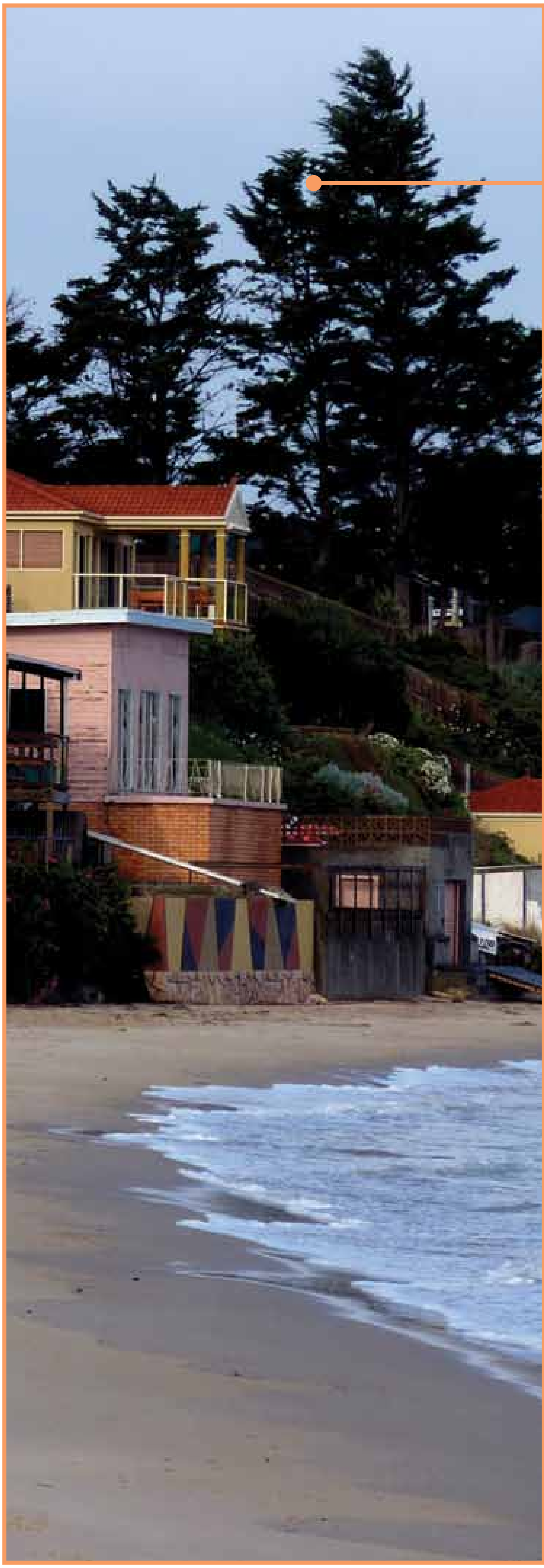

3 Methodology

Following McInnes et al (2009b, c), storm tide return levels are developed from separately-evaluated probability distributions of storm-surge heights and tide heights using an approach based on the Joint Probability Method (JPM) (Pugh and Vassie 1980; Tawn and Vassie 1989) as described in McInnes et al (2009b). The procedure for developing spatial maps of both surge and tide data is illustrated in Figure 7. After selecting a population of the most severe storm-surge events in the historical record, each event is simulated with a hydrodynamic model and the highest sea level attained at each gridpoint in the computational domain is stored for subsequent statistical analysis. For tides, amplitudes and phases of the main tide constituents are interpolated to the same computational grid as used for storm-surge modelling and a tide prediction model is then used to predict tides and calculate tide height frequency distributions.

3.1 Hydrodynamic model

The model used in this study is the two-dimensional hydrodynamic model, GCOM2D. This model solves the depth-averaged hydrodynamic equations for currents and sea levels. Details of the model formulation can be found in Hubbert and McInnes (1999). The model was set up over two regions shown in Figure 8. The grid defining the outer region, spanning much of southeastern Australia, had 5 km resolution while the inner grid over Tasmania and Bass Strait had 1 km resolution. Hourly sea-level heights and currents, simulated on the 5 km grid, were applied as lateral boundary conditions on the 1 km grid.

3.2 Data sources and model performance

Topographic and bathymetric data for the 5 km grid were obtained from the AUSLIG 9 second Digital Elevation Model (Geoscience Australia, 2008) and the Geoscience Australia (formerly AGSO) 30 second bathymetry data set. On the 1 km grid the 3 arc-second (~90 m) Shuttle Radar Topography Mission data was used over land from CGIAR-CSI (2008).

The simulation of storm surges requires that the hydrodynamic model be forced with near-surface winds (typically at 10 m above the surface) and sea surface pressure. There are two available sources of atmospheric reanalyses for the period from which the severe residual events from 1964 to 2002 were selected. The U.S. National Centers for Environmental

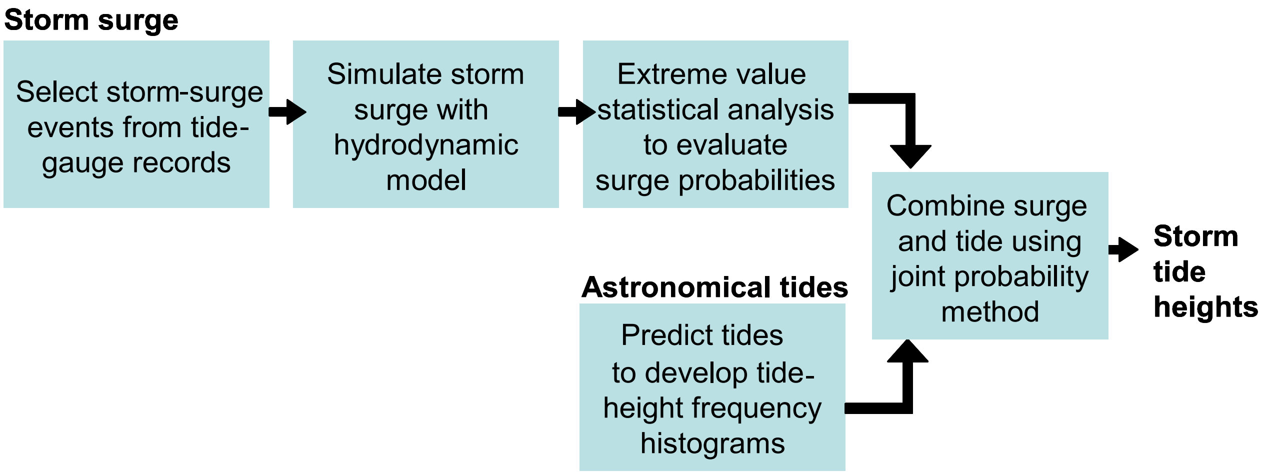

Figure 7: Schematic illustrating modelling approach used in this study.

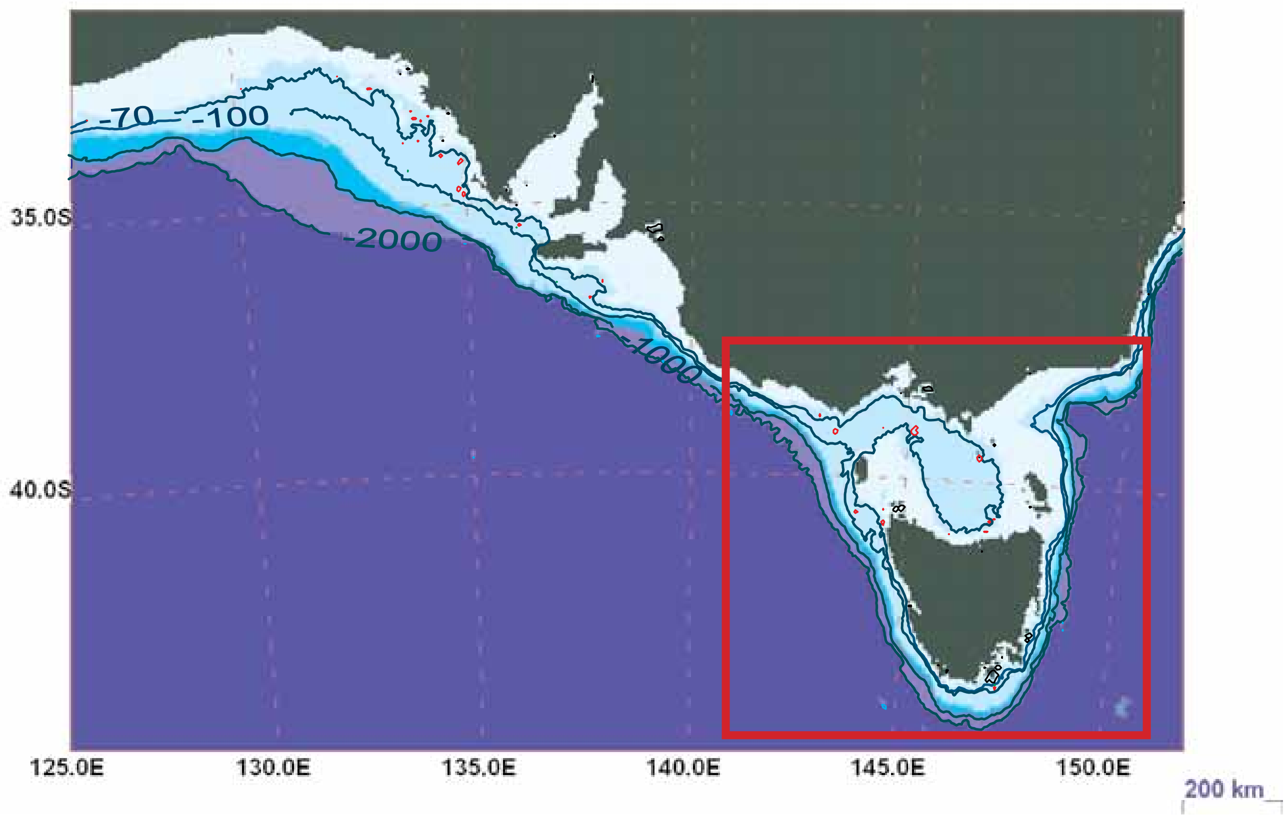

Figure 8: The two regions over which hydrodynamic simulations were performed. The outer region represents a 5 km horizontal resolution grid which was used to provide boundary conditions for the smaller grid centred over Tasmania and Bass Strait at 1 km resolution.

Prediction (NCEP) reanalyses (Kalnay et al 1996) and the European Centre for Medium-Range Weather Forecasts (ECMWF) ERA40 reanalyses (Uppala et al 2005). For NCEP, wind fields at 10 m above the surface were available on a 1.875 degree x1.875 degree global grid and the mean sea-level pressure fields were available on a 2.5 degree x2.5 degree global grid every 6 hours from 1948 onwards. For ERA40 wind and pressure data was available on a 2.5 degree x2.5 degree global grid from 1957 to 2002.

Both sets of atmospheric data were assessed in terms of their suitability for use as atmospheric forcing in the current study. Wind and pressure data were compared with hourly measured wind and pressure at Portland, Burnie and Spring Bay obtained from Bureau of Meteorology (2011) for approximately a 9 year period. Figure 9 summarises the agreement between measured data and simulations in the form of a Taylor diagram (Taylor 2000). A Taylor diagram represents, on a single figure, three quantities commonly used in the comparison of pairs of data series; correlation coefficient, normalised root mean square error, and normalised standard deviation. A perfect correlation between the model and observed time series would yield a point lying on the x-axis at the position of the open circle. A normalised standard deviation less than (greater than) 1 indicates a modelled time series that is smoother (noisier) than the observations. In terms of location, highest agreement is seen between reanalysis data and measurements at Portland while lowest agreement is seen at Burnie. For each location,

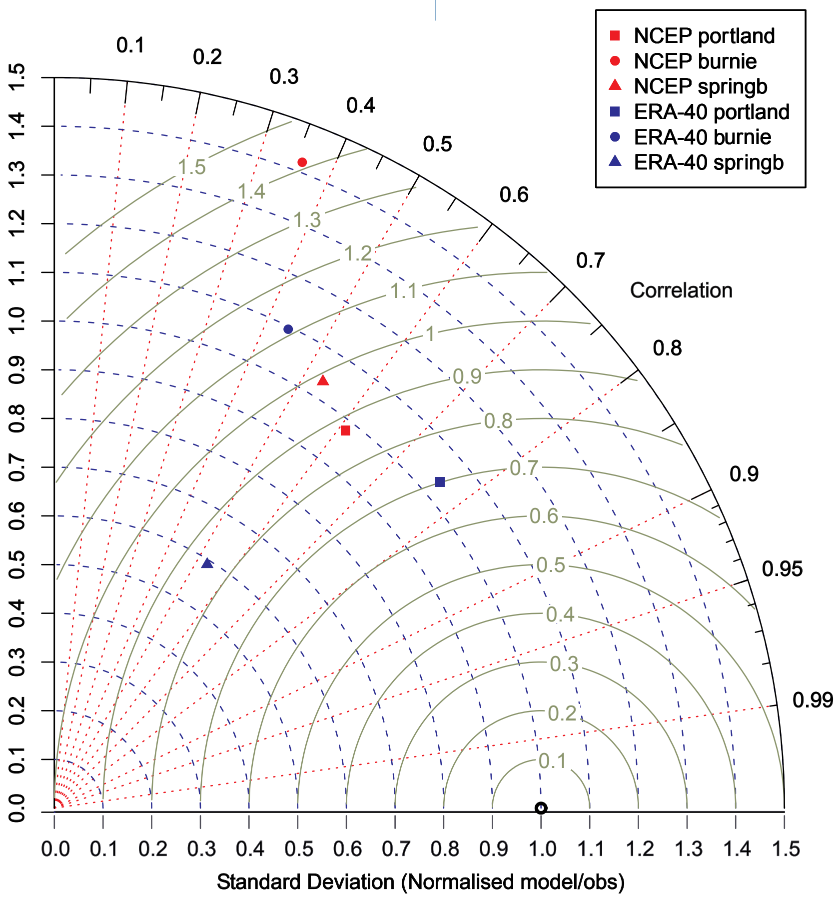

Figure 9: Taylor diagram representing agreement between time series of measured and reanalysis wind speed at Portland, Burnie and Spring Bay for both NCEP (red) and ERA40 (blue) reanalysis products. The radial co-ordinate gives the magnitude of total standard deviation, normalised by the observed value, and the angular co-ordinate gives the correlation with observations. The distance between the observed and modelled point is proportional to the RMS model error. The wind speed varies in amplitude between these three locations, and thus each time series has been normalised. Perfect correlation between the reanalysis winds (NCEP or ERA) and the observed winds would place these points on the horizontal axis. No correlation between the reanalysis and observed winds would place the points on the vertical axis. The distance from the origin indicates the difference in strength between the reanalysis and observed winds. For example, the NCEP Portland winds (red square) have almost the same signal variance as the observed winds (ie almost 1.0 on radial axis) with a correlation with the observed wind field of 0.6 and a RMS model error of 0.9. This can be contrasted with the ERA-40 wind field which is biased to a low level of variability compared with the observed winds, but still has a correlation of 0.5 and a RMS model error of 0.85.

ERA-40 data indicates closer overall agreement with measurements at all locations, exhibiting higher correlations and lower standard deviations and RMS errors compared to the NCEP data. On the basis of this comparison, ERA-40 reanalysis data were selected as forcing for the subsequent modelling in this study. To be applied to GCOM2D, the data were interpolated spatially to the hydrodynamic model grids.

The performance of the hydrodynamic model was assessed by carrying out month-long simulations from which performance statistics could be evaluated. On the basis of the time series of daily maximum residuals compiled in Section 2, the months of May 1994, November 1994, September 1999 and June 2002 were selected as months in which high sea-level residual events occurred, and so were selected for simulation. Figure 10 and Figure 11 compare the time series at five tide gauge locations around Victoria and Tasmania for November 1994 and September 1999 respectively. These indicate that the model reasonably reproduces the major residual peaks, although there is a tendency for the model to overestimate the smaller amplitude events and some phase errors are evident between simulated and observed peaks towards the end of the month, particularly at Spring Bay and Burnie. Figure 12 summarises the model performance in a Taylor diagram over the four-month-long simulations. The closest agreement between simulations and observations is seen at Stony Point and Portland, all of which have the highest correlation and lowest RMS error and a normalised standard deviation closest to 1. The poorest agreement is seen at Burnie and George Town.

As discussed earlier, the preferred approach to use in this study is to model the surges and tides separately and statistically combine the two to evaluate extreme sea levels. However, coastal currents induced by astronomical tides and meteorological forcing can interact non-linearly such that the sea-level heights obtained from the combined forcing of tides and meteorology does not equal the height of tides and meteorology derived separately, and subsequently summed together. This non-linear interaction is generally strongest over broad and shallow continental shelves, where the retarding effect of bottom friction more effectively influences the currents because of the large fluctuation in the ratio of current speed to water depth. This has been noted around the UK coast (eg Horsburgh and Wilson 2007) and the northwest Atlantic (Bernier and Thompson 2006). To determine the importance of non-linear effects, an additional two sets of month-long simulations were conducted. In the first, both tidal and meteorological forcing were applied to the model simulation yielding time series of sea-level height. Tidal forcing was applied to the hydrodynamical model by predicting the tide height on the lateral boundaries of the model grid using tide constituents from the Australian Bureau of Meteorology's *National Tidal Centre* regional tide model (James Chittleborough, pers. comm.) that were available on a 5'x5' lat/long grid over Australia's surrounding oceans. The second set of simulations contained tide forcing only, producing a time series of sea-level heights. Subtracting the tide only simulation from the simulation with both meteorological and tide forcing yields a time series of sea-level residuals that explicitly includes the contributions from the interactions of tidal and meteorological forcing. These were compared with the time series from a third simulation, with meteorological forcing only, at several locations around Tasmania and found to show close agreement, as illustrated in Figure 13 for Spring Bay. The similarity between the two time series indicates that the separate treatment of tides and surge in this study is valid along this coastline.

3.3 Storm-surge simulations and probabilities

For the purposes of evaluating storm-surge probabilities, the population of sea-level events identified in Section 2.3 was simulated, and the peak sea level at each grid point from each simulation was stored for later analysis. Since the population of events identified in the tide-gauge records represented only a 38 year period, extreme-value statistical methods were applied to evaluate probabilities of events rarer than those seen in the observational record.

Two commonly used distributions for extremes data are described in Coles (2001). The first of these is the Generalised Extreme Value distribution (GEV), which is applied by dividing a time series of data into equal time intervals (usually yearly time intervals), selecting the maximum data value for each time interval and fitting the distribution to the set of maximum values (a block maxima approach). The second of these is the Generalised Pareto Distribution (GPD), which is fitted to a sample of values in a data set that exceed a chosen high threshold (a points-over-threshold approach). The suitability of these approaches was investigated by McInnes et al (2009b). It was found

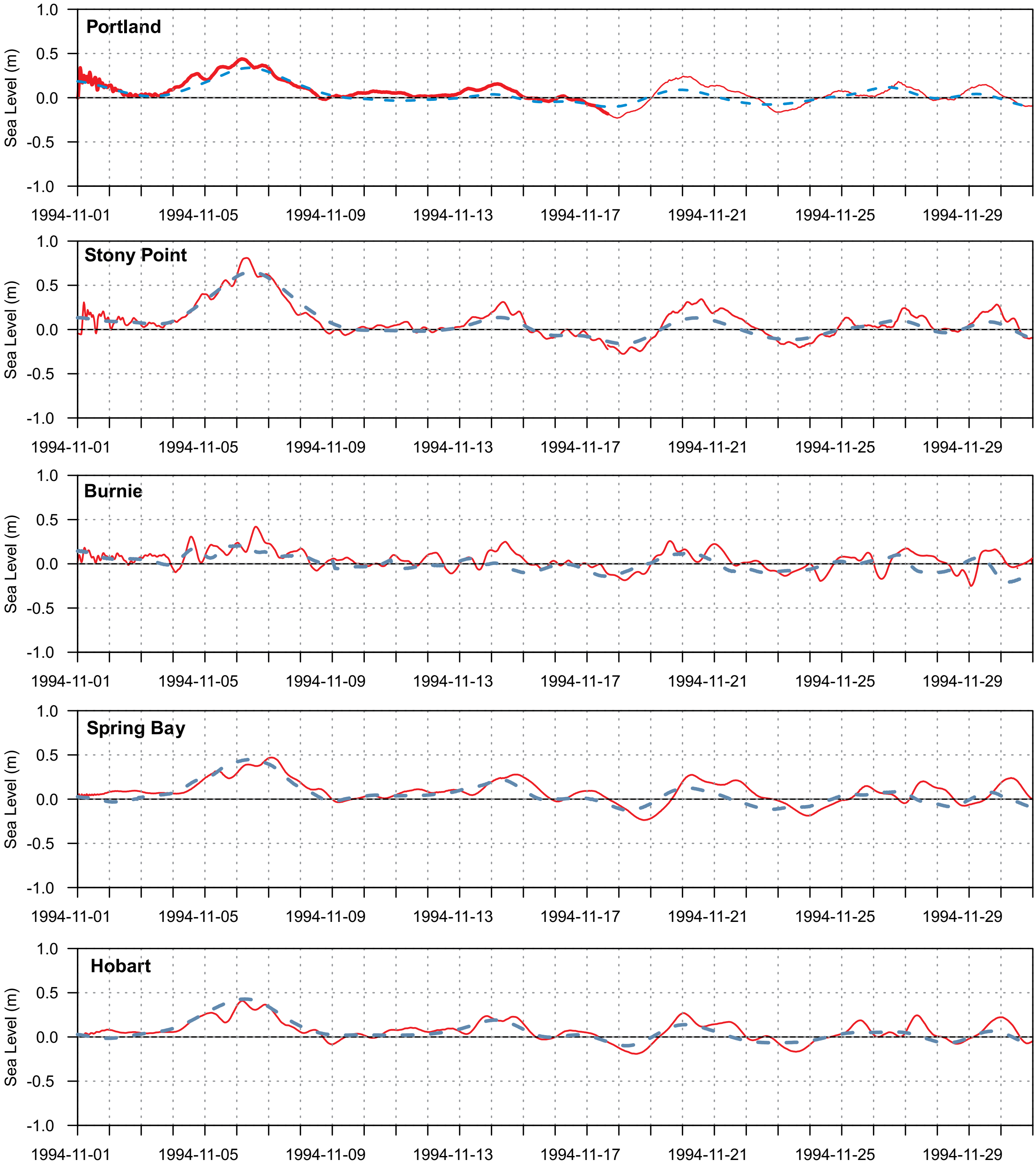

Figure 10: Comparison of sea-level residuals calculated by filtering astronomical tides from the measured sea levels at the tide gauges indicated (blue dashed curve) and modelled residuals (red curve) obtained by forcing the hydrodynamic model with the ERA-40 reanalysis data for November 1994.

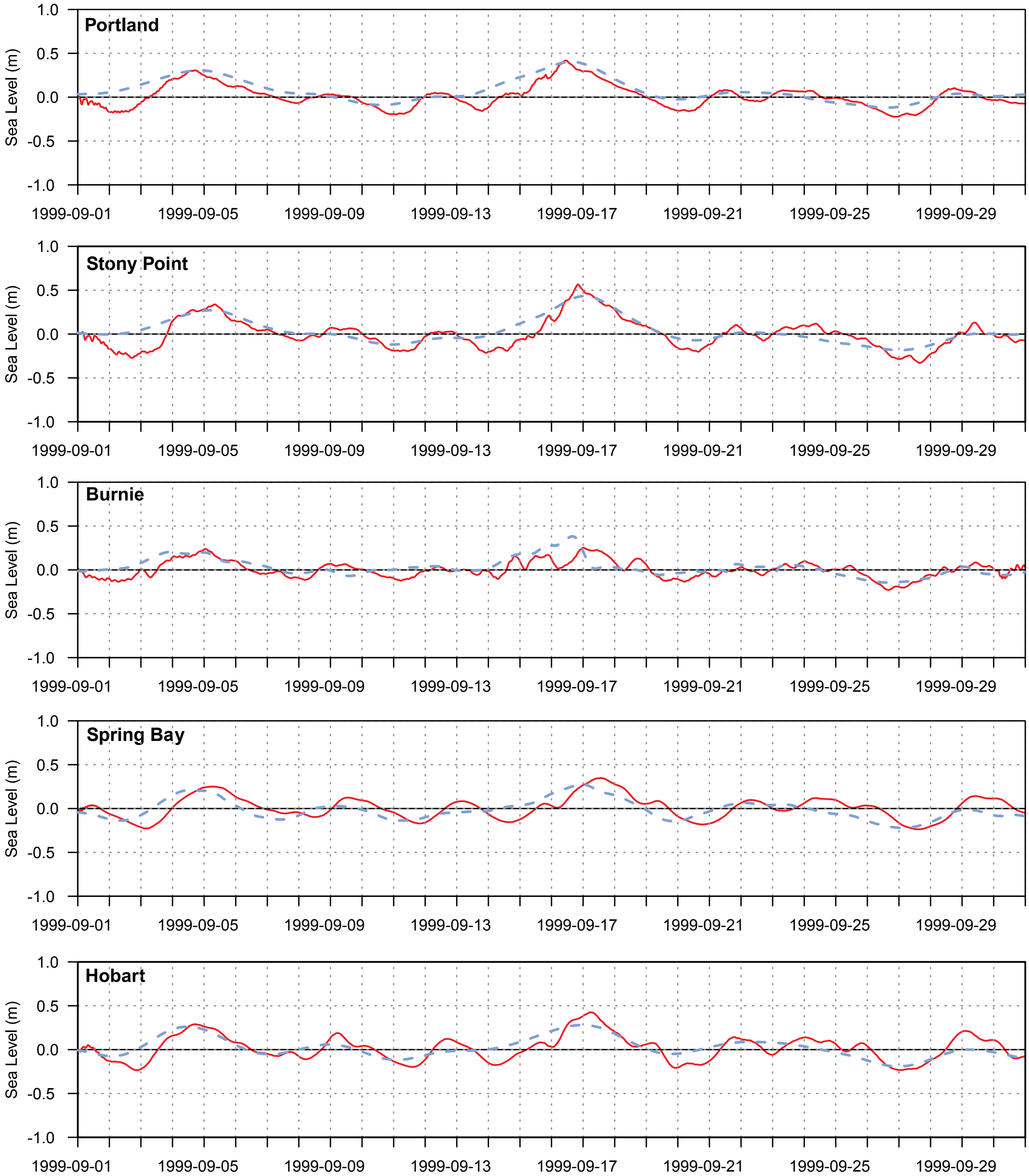

Figure 11: Comparison of sea-level residuals calculated by filtering astronomical tides from the measured sea levels at the tide gauges indicated (blue dashed curve) and modelled residuals obtained by forcing the hydrodynamic model with the ERA-40 reanalysis data for September 1999.

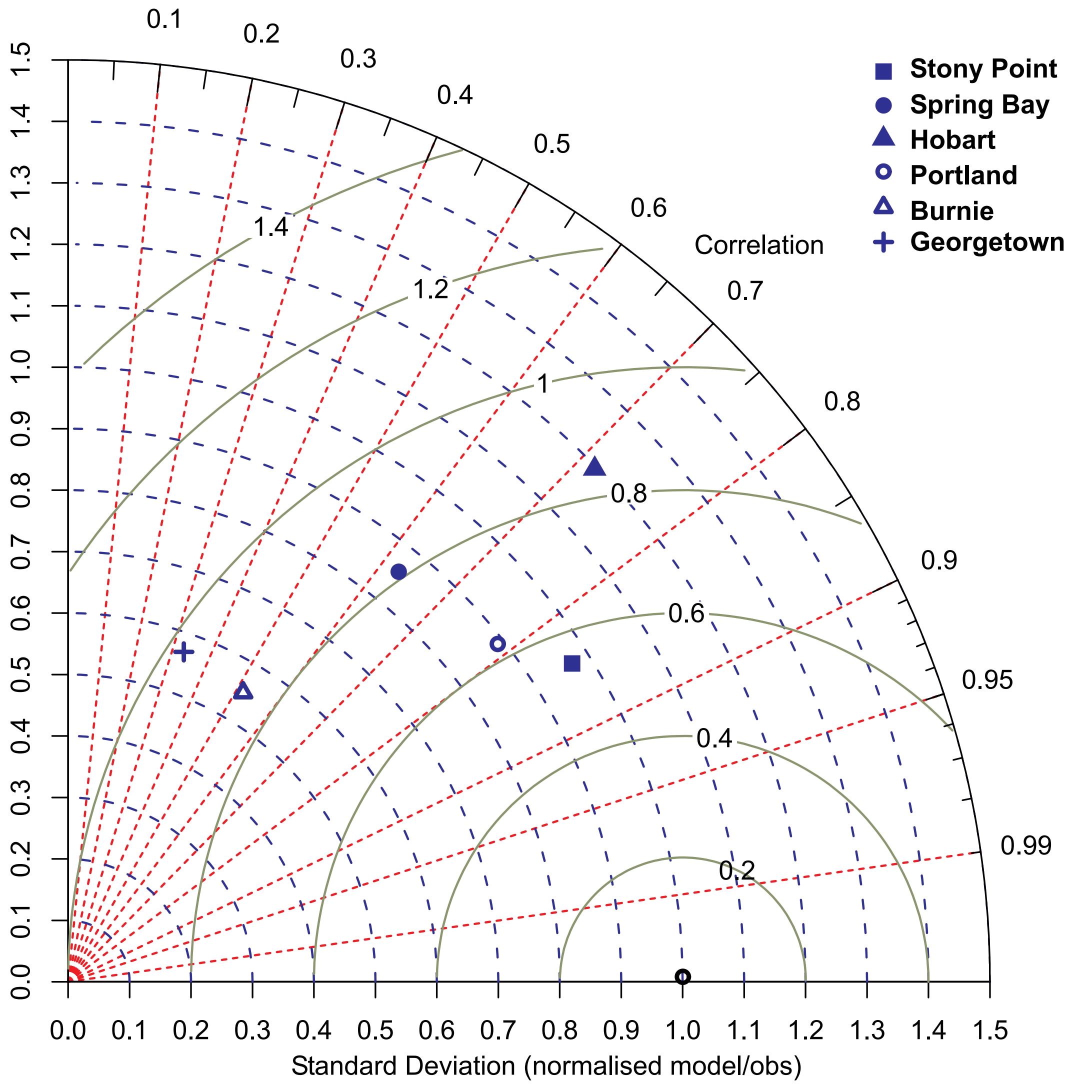

Figure 12: Taylor diagram representing agreement between time series of sea-level residuals derived from observations and model simulations. See caption of Figure 9 for an example on the interpretation of points on a Taylor diagram.

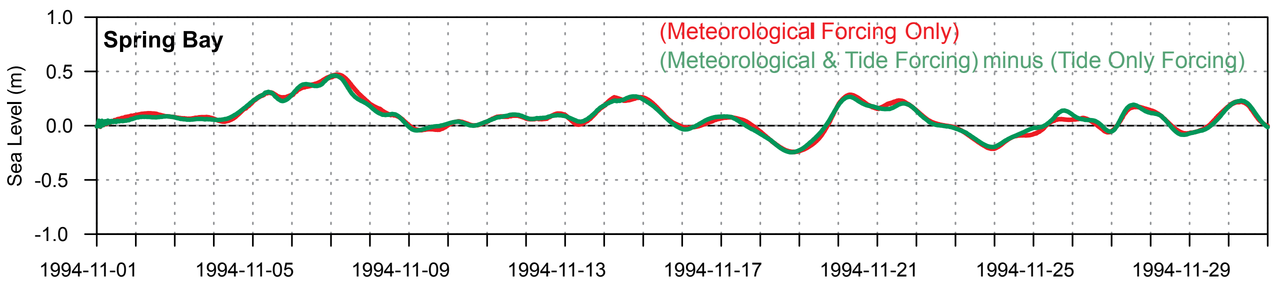

Figure 13: Time series representing agreement between time series of model sea levels obtained from meteorological forcing only and those obtained from tide only simulations subtracted from tide and meteorological forcing.

that the application of the GPD was problematic because of the difficulty in automating the process of selecting an appropriate threshold for the sample of extreme values to be fitted. On the other hand, the GEV approach, while easier to apply, is wasteful of information when more than one extreme value occurs in each year. A variation on the GEV approach is the *r* largest GEV approach (see Coles 2001), in which the *r* largest values per year are used in the fitting procedure. This approach was adopted in the present study. Goodness-of-fit diagnostic diagrams (see Coles 2001) were generated and inspected for a well-distributed sample of locations in each model grid for r values ranging from one to six. It was concluded that goodness-of-fit statistics were maximised when the six largest events per year were selected and so this method was employed in the present study.

3.4 Tide probabilities

The periodic behaviour of the tides at a particular location can be determined from a set of constants referred to as tidal constituents. These provide the phase and amplitude of variations in the tide-producing forces. Knowledge of these constants allows tidal behaviour to be predicted and tide height frequency distributions suitable for input to the JPM to be generated. For the purpose of developing spatial maps of tide height, tide constants for the four leading semi-diurnal tide constants (M2, S2, N2, K2) and the four leading diurnal constants (O1, P1, Q1, K1) were obtained from the Australian Bureau of Meteorology's National Tidal Centre regional tide model (James Chittleborough, pers. comm.) on a 5 degree x 5 degree lat/long grid over Australia's surrounding oceans (Figure 14). These were interpolated to the 1 km Tasmanian grid. For each ocean grid point, the tidal model of Foreman (1977) was used to predict the tides every 15 minutes over an 18.6 year period. The predicted tide heights were then binned to produce a tide-height frequency distribution. Figure 15 compares tide-height frequency distributions and cumulative frequency distributions obtained from predicting the tides using the eight constituents from the National Tidal Centre tidal model with those predicted using a larger range of tide constants published in the Australian Tide Tables (2007). Figure 15 demonstrates the difference in tidal characteristics around the Tasmanian coast. For example, the marked bi-modal distribution at Burnie results from this location having a semi-diurnal tidal range (two high tides and two low tides per day). The distribution of tide heights at

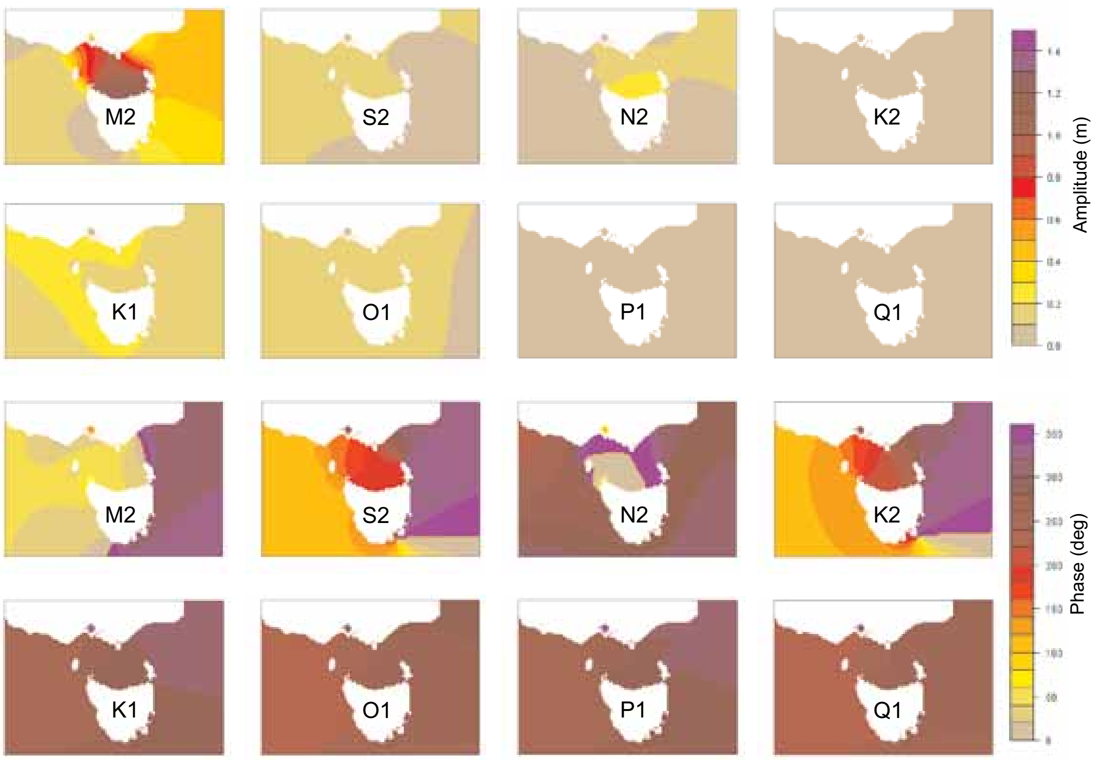

Figure 14: Amplitudes and phases of the leading semi-diurnal tide constituents (top two rows) and diurnal tide constituents (bottom two rows) used to develop tide height frequency distributions.

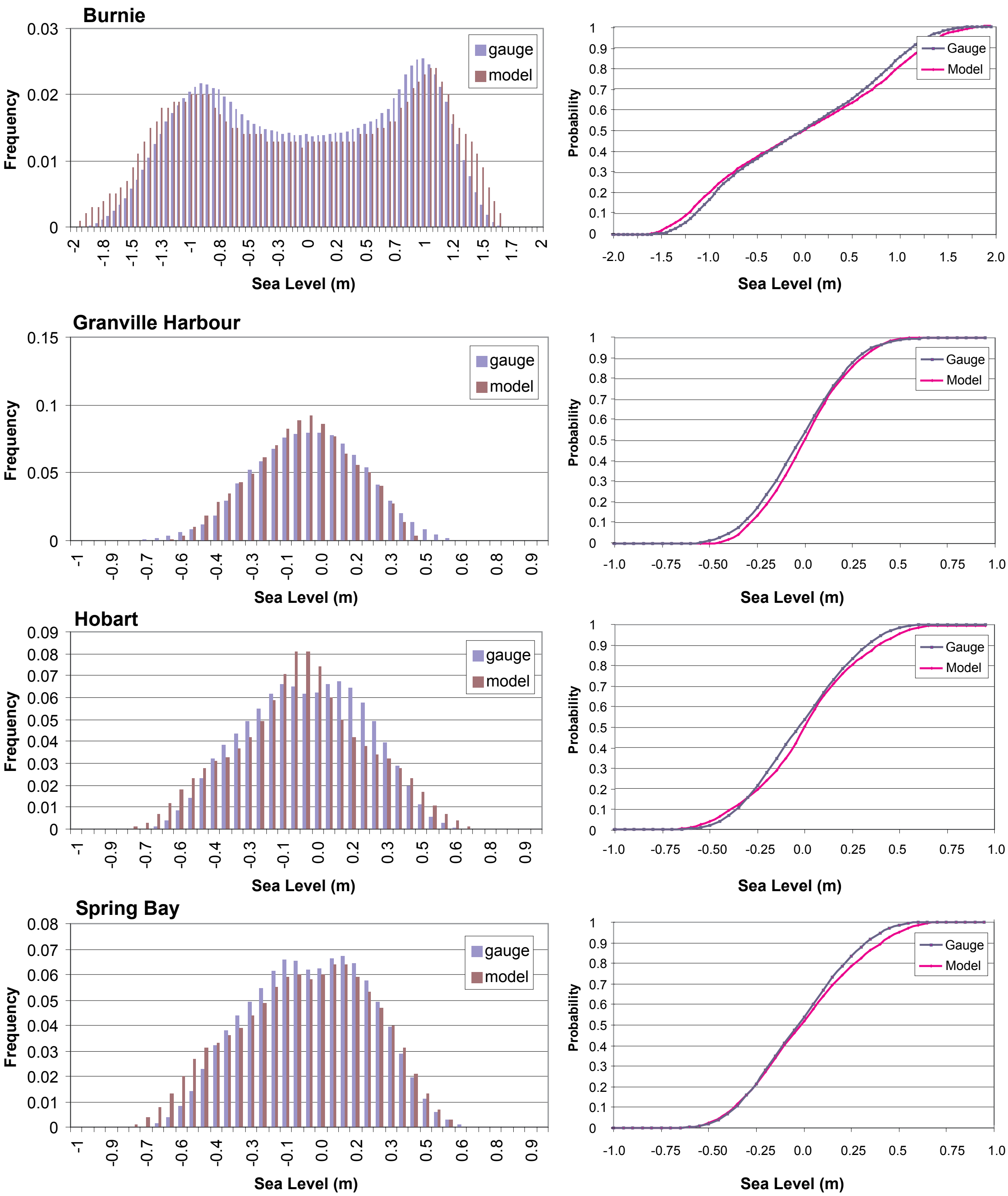

Figure 15: Tide height frequency distribution (left) and cumulative frequency curve (right) for the locations listed.

Granville Harbour on the other hand is representative of this location having a diurnal tidal range (one high and one low tide per day).

3.5 Evaluation of storm tide return periods

Pugh and Vassie (1980) describe an approach, commonly referred to as the JPM, for combining the probability distributions of tide and storm-surge to estimate return periods of the combination of the two. The approach used in this study is similar to the Revised Probability Approach described by Tawn and Vassie (1989) in that the surge distribution is represented by fitting the modelled surges to a GEV distribution. This allows the evaluation of return periods for observed extremes and the extrapolation to longer return periods and larger extremes than those represented in the historical record. The combination of the two probability distributions is achieved by randomly sampling a population of tide and surge values from storm-surge and tide probability distributions estimated following the method described in the previous two sections, and summing them to develop a population of storm-tide-heights. Return periods for storm tide heights were estimated by ranking the sampled storm tides from largest to smallest and assigning the return period to the event height according to $R = N / r$, where R is the return level, N is the number of random samples and r is the rank of the event. To estimate the uncertainty in the storm tide estimates, 200 sets of 10,000 storm tides were sampled and each set of 10,000 storm tides was ranked from largest to smallest. From the 200 values associated with each rank (highest, second highest and so on), the mean was taken to represent the best estimate storm tide height, and the standard deviation was taken to represent the uncertainty associated with the random sampling.

For the purposes of validating the results of the modelling approach for generating storm tide return periods, extreme-water return periods are also calculated by fitting a GEV to a set of extreme total water levels selected from tide-gauge observations. Extreme sea-level events were selected from approximately 20 years of data from Spring Bay and 34 years of data from Burnie, George Town and Hobart. The data was filtered to remove low-frequency oscillations such as seasonal and longer period oscillations and detrended to remove the effect of sea-level rise. Event peaks were declustered by ensuring a separation between peaks of at least 48 hours. Goodness-of-fit diagnostic diagrams (Coles, 2001) were generated for r values ranging from one to six highest events per year and the goodness-of-fit statistics were found to be maximised when the two largest events per year were selected. The results of these calculations are given in Table 2.

3.6 Estimation of uncertainties

In addition to the uncertainty in storm tide return levels due to the random sampling of tide and surge heights, three other significant types of uncertainty were taken into account. These were the uncertainty due to imperfections in the representations of storm surges by the hydrodynamic model (including the model itself and the atmospheric forcing conditions), the uncertainty due to imperfections in the representation of tides by the tide prediction model and tidal constituent data, and the uncertainty associated with the statistical fits to the extreme surge heights.

We derived 95% confidence intervals in estimated storm tide return levels that accounted for these potential sources of error (see Table 2). Standard errors were estimated for each identified uncertainty and combined using $DX=\sqrt{(\Sigma(DX_k)^2)}$, where k=1, N represents the sources of uncertainty. For storm surges, errors between modelled and observed surge peaks were estimated at each location and ranged from ±0.08 m across all surge peaks at all locations. It is assumed that 95% of the errors for the modelled storm surges fall within ±0.08 m and hence 0.08 m corresponds to 1.96 standard errors and so one standard error is 0.04 m. For each tide gauge, a standard error was obtained by calculating the root-mean-square difference between the model and gauge derived tide heights and these ranged from 0.05-0.07 m. Next we divide the 95% confidence limits on the statistical estimates for storm-surge return levels by 1.96 and add the resulting standard errors to the formula. Finally we incorporate the standard errors estimated for the joint probability sampling of tide and surge heights and use the combined error formula to evaluate a standard error for the storm tide return levels. These standard errors are reported in Table 2 for current climate storm tide estimates. We expect the same modelling and statistical fitting uncertainties to be broadly applicable to the storm-tides calculated for each individual future climate scenario considered.

				Sea Level Rise (m) for given year, for A2 emissions scenarios (Nakićenović and Swart 2000)						
				2030		2070		2090		
	Return Period (years)	Return Level (obs) (m)	Return Level (model) (m)	5% 0.047	95% 0.139	5% 0.142	95% 0.401	5% 0.203	95% 0.588	95% +wind 0.588
Stanley*	10		1.72 ±0.08	1.77	1.86	1.86	2.26	1.92	2.31	2.30
	20		1.77 ±0.08	1.81	1.90	1.91	2.31	1.97	2.35	2.35
	50		1.81 ±0.08	1.86	1.95	1.95	2.35	2.01	2.40	2.39
	100		1.84 ±0.08	1.89	1.98	1.98	2.38	2.04	2.43	2.42
Burnie	10	1.84 ±0.02	1.80 ±0.07	1.85	1.94	1.94	2.34	2.00	2.39	2.38
	20	1.86 ±0.03	1.85 ±0.08	1.89	1.99	1.99	2.39	2.05	2.44	2.42
	50	1.87 ±0.03	1.90 ±0.08	1.94	2.03	2.04	2.44	2.10	2.48	2.47
	100	1.88 ±0.04	1.92 ±0.08	1.97	2.06	2.07	2.46	2.13	2.51	2.50
Devonport*	10		1.82 ±0.08	1.86	1.95	1.96	2.36	2.02	2.40	2.39
	20		1.86 ±0.08	1.91	2.00	2.00	2.40	2.06	2.45	2.44
	50		1.91 ±0.08	1.96	2.05	2.05	2.45	2.11	2.50	2.49
	100		1.94 ±0.08	1.99	2.08	2.08	2.48	2.14	2.53	2.52
George Town	10	1.89 ±0.03	1.87 ±0.09	1.92	2.01	2.02	2.41	2.08	2.46	2.45
	20	1.91 ±0.04	1.92 ±0.10	1.97	2.06	2.07	2.46	2.13	2.51	2.50
	50	1.94 ±0.05	1.97 ±0.10	2.02	2.11	2.12	2.51	2.18	2.56	2.55
	100	1.96 ±0.07	2.00 ±0.11	2.05	2.14	2.15	2.54	2.21	2.59	2.58
Bicheno*	10		0.93 ±0.07	0.93	1.02	1.02	1.42	1.08	1.47	1.46
	20		0.97 ±0.07	0.96	1.05	1.06	1.45	1.12	1.50	1.50
	50		1.01 ±0.07	1.00	1.09	1.09	1.49	1.15	1.54	1.54
	100		1.04 ±0.07	1.02	1.11	1.11	1.51	1.17	1.56	1.56
Spring Bay	10	0.99 ±0.04	0.89 ±0.07	0.93	1.03	1.03	1.43	1.09	1.47	1.47
	20	1.01 ±0.05	0.92 ±0.07	0.97	1.06	1.07	1.46	1.13	1.51	1.51
	50	1.04 ±0.07	0.96 ±0.07	1.01	1.10	1.10	1.50	1.16	1.55	1.55
	100	1.05 ±0.08	0.99 ±0.07	1.03	1.13	1.13	1.53	1.19	1.57	1.58
Hobart	10	1.12 ±0.05	1.14 ±0.08	1.19	1.28	1.29	1.68	1.35	1.73	1.73
	20	1.16 ±0.07	1.20 ±0.09	1.24	1.33	1.34	1.74	1.40	1.78	1.78
	50	1.21 ±0.09	1.25 ±0.10	1.30	1.39	1.40	1.79	1.46	1.84	1.83
	100	1.24 ±0.11	1.29 ±0.11	1.34	1.43	1.43	1.83	1.50	1.88	1.87
Granville Harbour*	10		0.70 ±0.07	0.75	0.84	0.84	1.24	0.91	1.29	1.29
	20		0.73 ±0.07	0.78	0.87	0.87	1.27	0.93	1.32	1.32
	50		0.76 ±0.07	0.81	0.90	0.90	1.30	0.96	1.35	1.35
	100		0.78 ±0.08	0.83	0.92	0.92	1.32	0.98	1.37	1.37

Table 2: Storm tide return periods for various locations around the Tasmanian coast evaluated on the basis of modelled extreme sea levels and with the projected range of A2 sea-level rise scenarios for 2030, 2070 and 2090. The final column includes both sea-level rise and wind speed change simulated by the GFDLCM 2.0 model. Sea levels are relative to Australian Height Datum (AHD) except at locations indicated by * where they are relative to mean sea level.

4 Future climate conditions

The impact of future extreme sea-level events will increase as mean sea-level rises. However, changes in the characteristics of extreme sea-level events may also change with changing meteorological forcing. In this section, an investigation of the changes to extreme events due to both wind speed changes and mean sea-level rise is undertaken.

4.1 Changes to wind speed

Storm-surge events tend to occur most commonly as a result of the winds associated with the passage of mid-latitude low pressure systems and their associated cold fronts. The Climate Futures for Tasmania simulations that downscaled the CSIRO-MK 3.5, GFDL 2.0 and GFDL 2.1 GCMs over Australia at around 50 km resolution (see Corney et al 2010 and McGregor and Dix 2008 for details of the model simulations) were investigated by Hemer et al (2010). In general the average change between 1981-2000 and 2081-2100 in east-west and north-south component wind was small for all models at Tasmanian latitudes. Between 40 degrees S and 45 degrees S at 150 degrees E, the mean westerly wind component strengthened by around 0.6-0.8 ms^{-1} and this change was marginally larger in the Climate Futures for Tasmania simulation forced by the GFDL2.0 GCM. Therefore this simulation was selected as the basis for investigating changes to winds and storm-surge-induced extreme sea levels. Windroses for climate model winds over 1981-2000 and 2081-2100 for summer (DJF) and winter (JJA), are shown in Figure 16, at selected locations. In summer, southerly to easterly component winds undergo an increase in frequency whereas westerly to southwesterly winds mostly undergo a decrease in frequency. In winter, southwesterly winds undergo a decrease while westerly and northwesterly winds undergo an increase. On the coast of mainland Australia during summer there is an increase in southerly and southeasterly winds and a decrease in southwesterly and westerly winds, while in winter there is an increase in northerly and northwesterly winds and a decrease in westerly and southwesterly winds.

The approach used to investigate the effect of wind speed changes on storm surges was to apply the changes in wind from 1981-2000 to 2081-2100 in the climate model to the observed winds used to force the storm-surge model. We refer to this method as the 'baseline perturbation method' to develop future projections. An alternative approach is the direct method in which the climate model winds are applied as forcing over historical and future time periods and the differences between the simulations of the two periods are calculated. Hemer et al (2010) applied both the baseline perturbation method and the direct method, the latter implemented both with and without bias correction applied to the winds, to develop projections of wave climate over eastern Australia. The three methods yielded broadly consistent changes in wave climate despite differences in the representation of present and future wave climates resulting from all three methods. The application of the direct method was beyond the scope of the present study because it required carrying out continuous multi-year simulations whereas the baseline perturbation technique required only that the pre-selected events identified in the historical record be adjusted to represent future winds. A downside of this approach is that it does not capture potential changes in frequency of storm-surge generating systems, only intensity changes to those events already identified. However, in the *r*-largest GEV approach used to analyse the storm-surge peaks where a constant number of events (*r*-events) per year are selected for analysis, a change in frequency could, in fact, only alter the extreme value fit to the population of events through a change to the magnitude of the *r*-largest events.

The differences in winds were calculated using the bivariate quantile adjustment procedure described by Hemer et al (2010) in which a joint probability distribution of the differences in eastward (u) and northward (v) wind components is evaluated between the 1981-2000 and 2081-2100 intervals and these differences used to adjust the observed winds. The procedure involves distributing, for each season, the u component winds into percentile bands and then within each percentile band of u, distributing v into percentile bands. A matrix of percentile differences between the time periods is then calculated. These changes are then applied to the events selected in Section 2.3 by adjusting the ERA40 winds into percentile bins for u and v for each season and applying the seasonal percentile differences. These adjusted winds were then used to

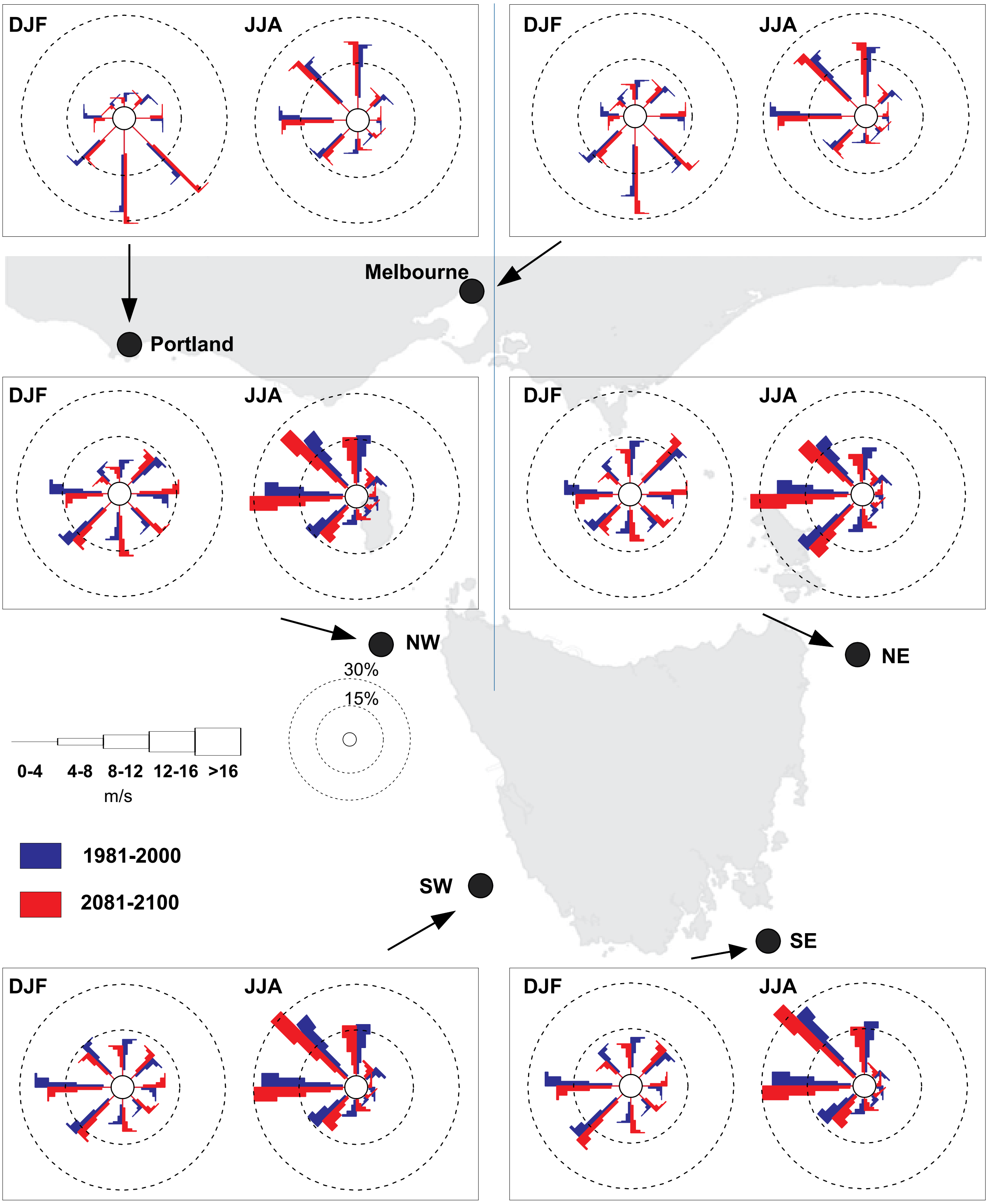

Figure 16: Histograms showing wind speeds for summer and winter over the 1981-2000 and 2081-2100 period from the Climate Futures for Tasmania simulations forced with the GFDLCM 2.0 model under the A2 scenario at the locations indicated.

4.2 Future sea-level rise

Using a number of emissions scenarios (Nakićenović and Swart 2000) the IPCC (2007) developed a range of plausible sea-level rise projections for 2090-2099, relative to 1980-1999. The simulations projected a rise of 0.23-0.51 m with an additional 0.1-0.2 m allowance for possible future dynamical changes in ice flow. These values have been interpolated by Hunter (2010) to the intervening decades of the 20th century. For consistency with the scenario used to force the Climate Futures for Tasmania simulation from which wind speed projections were obtained for 2081-2100 relative to 1981-2000, we consider the A2 (high emission scenario) sea-level rise scenarios for 2090 relative to 1990. The projected range of sea-level rise allowing for the additional rapid response of the ice sheets, is 0.20-0.59 m. For comparison of the relative response of projected wind speed changes and sea-level rise we take the upper limit of this range, rounded to 0.6 m to be consistent with our choosing of the simulation with the largest wind speed response. However, we also consider the impact of the full range of projected sea-level rise from Hunter (2010) for the A2 scenario for 2030 (0.05-0.14 m) and 2070 (0.14-0.40 m) as well as 2090 without consideration of wind speed change.

5 Results

5.1 Current climate

Figure 17a and Figure 17b show the 99th percentile height associated with the modelled storm-surge and the tide-height distribution. Storm surges are relatively small and range from 0.2-0.4 m around the coastline in the north of the state. Larger values up to 0.7 m occur along the southeast coastline. In contrast, tide heights show a range of up to 1.6 m along the north coast, 0.5-0.7 m on the east coast and 0.4-0.5 m on the west coast of Tasmania. Strong tide height gradients occur in the northeast and northwest of the state. The estimated one-in-100 year storm tide height is shown in Figure 18. The highest values of between 1.9 and 2.0 m occur on the Tasmanian north coast, owing to the large tidal range within Bass Strait. The larger storm surges found to occur along Tasmania's southeast coast contribute to one-in-100-year ARI storm tides of 1.2 to 1.4 m.

Table 2 (page 28) presents values for a selection of locations and their estimated uncertainties. Comparison of the modelled return periods with those obtained by fitting a GEV to available data reveals that the modelled and observed return periods show reasonably close agreement with the modelled values generally within about 0.04 m of the values estimated from the tide-gauge data. The exception is Spring Bay for which modelling values appear to be lower by a larger amount. The reasons for this are uncertain but may relate to the shorter record for Spring Bay.

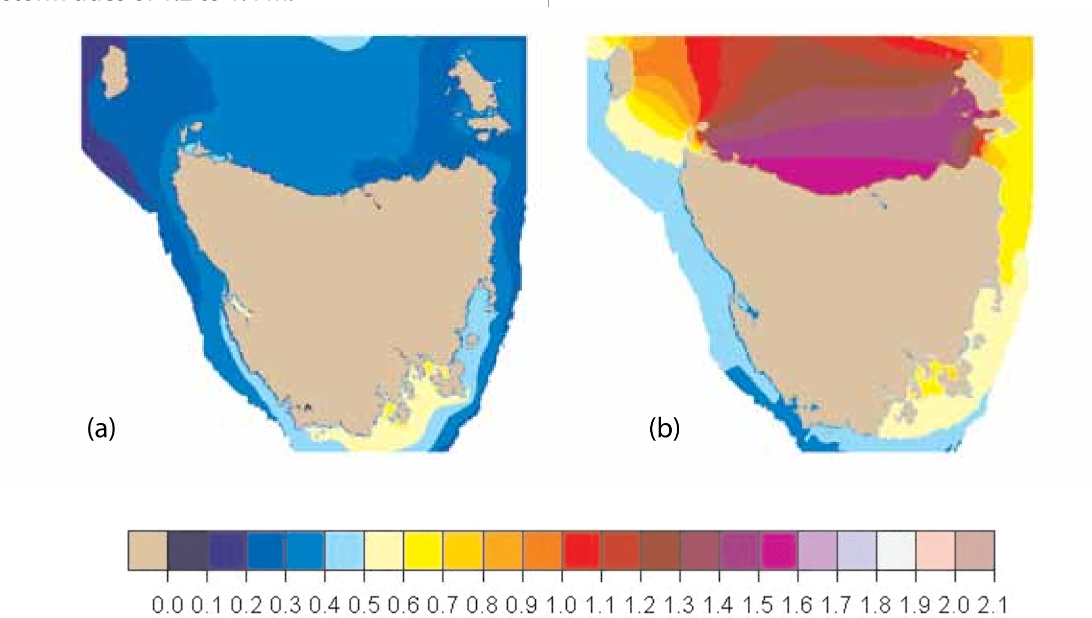

Figure 17: (a) 99th percentile surge height and (b) 99th percentile tide height (units are m and relative to mean sea level).

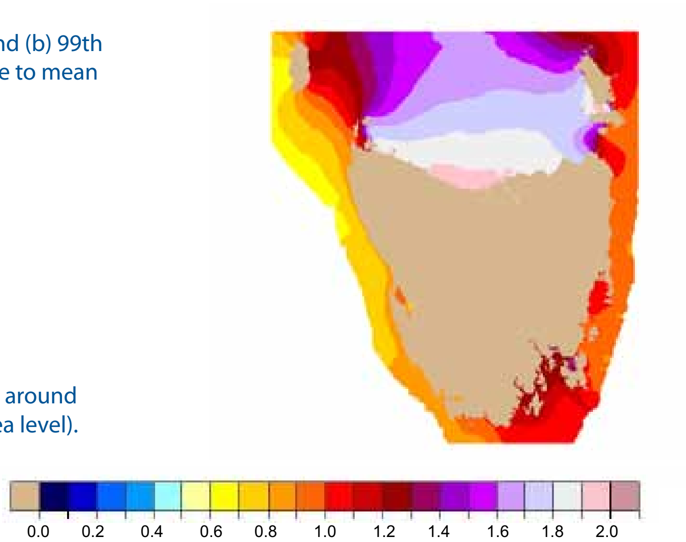

Figure 18: One-in-100 year storm tide height around Tasmania (units are m and relative to mean sea level).

5.2 Future climate conditions

Figure 19 shows the ARIs for storm tides at several locations around the Tasmanian coast evaluated on the basis of late 20th century conditions and for 2030 and 2090, relative to the late 20th century values. The results are based on high-end estimates of sea-level rise for the A2 emissions scenario reported in Hunter (2010). These show that a sea-level height that is likely to be exceeded on average once every 100 years in Hobart may be exceeded every 10 to 20 years by 2030 and more frequently than once every five years by 2090. In George Town a sea-level height that is likely to be exceeded on average once every 100 years may be exceeded every 10 to 30 years by 2030 and more frequently than once every five years by 2090. The values for selected locations and return periods are also presented in Table 2.

As can be seen in Figure 19 and Table 2, changes in wind speed have a negligible effect on storm tide return periods, demonstrating mainly no change or slight decrease in sea level. While seeming somewhat contrary to the wind change results, this appears to occur because winds in the future climate undergo increasing strength and frequency in some wind speed and direction classes but these are being cancelled out by decreasing strength and frequency in others (for example an increase in strong westerlies and northwesterlies and a decrease in southerlies and southwesterlies in winter at points around Tasmania). Furthermore, there is a tendency for weakening winds particularly from the west and southwest along the coastline of mainland Australia. Previous studies have demonstrated that the storm-surge magnitude along the Victorian coast is strongly influenced by the storm-surge response further westward as the storm surge propagates as a wind-forced coastally trapped wave (e.g. McInnes and Hubbert 2003). A weakening of the storm surge in this region due to decreases in wind strength may be influencing the overall storm-surge response along the Tasmanian coast despite the strengthening of local winds in some direction classes. A more comprehensive investigation of the results found here is beyond the scope of the current study but will be investigated further in future work. Future sea-level rise on the other hand will increase the frequency of extreme sea-level events. With sea-level rise, a given water level will be exceeded more frequently since progressively less severe conditions will be required to exceed that water level threshold. By 2030, under a low end sea-level rise scenario, the sea levels associated with a one-in-100 year event will more than double in frequency while under the high end sea-level rise scenario, they will increase by a factor of 10 or more (Figure 19).

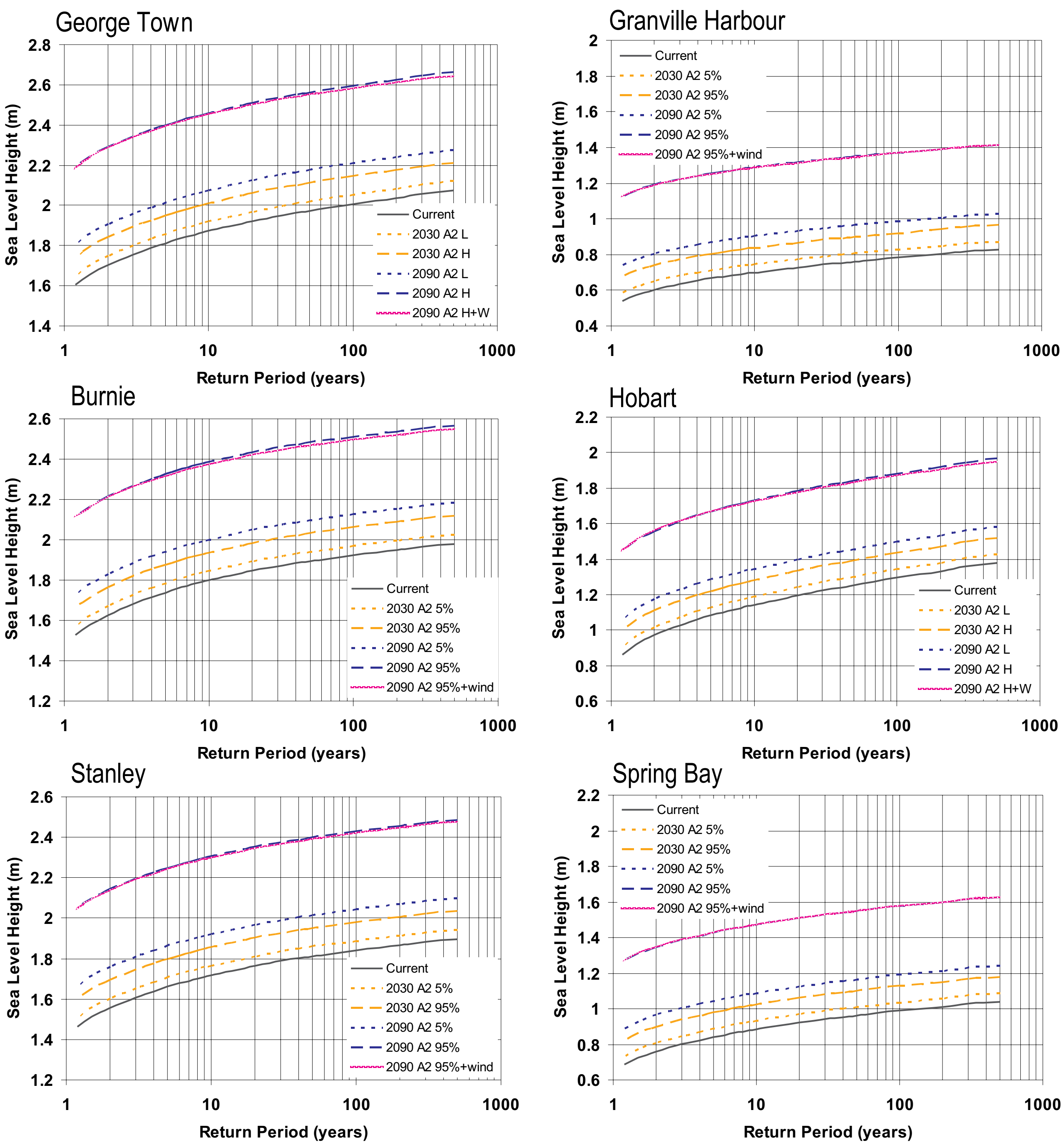

Figure 19: Return period curves at several locations around Tasmania. (Sea levels are AHD except for Stanley and Granville Harbour where they are relative to mean sea level).

6 Summary and Conclusions

Rising mean sea levels will be felt most acutely through the occurrence of extreme sea-level events such as those caused by storm surges. To provide a basis for investigating the impacts of future sea-level rise, the main objective of this study was to evaluate return periods of extreme sea levels around the Tasmanian coast under late 20th century conditions. An investigation of the changes in storm tides due to wind and sea-level changes was also carried out.

The causes of storm surges were investigated and it was found that west to east moving cold frontal systems associated with a low pressure centre to the south of Tasmania were the main cause of elevated sea levels on the southeastern coastline. On the northern Tasmanian coastline an increase in the non-tidal component of the sea level was found to be most commonly associated with a low pressure centre located to the west of Tasmania or in Bass Strait, which causes strong northerly winds on this coastline.

The methodology used to evaluate storm tide return periods exploited the finding that extreme sea levels along the Tasmanian coast are highly correlated with those on the southern mainland coast so that events in a small number of tide-gauge records of several decades in length could be used to identify extreme sea-level events that have affected the Tasmanian coast over this time. These events were then hydrodynamically modelled to generate spatially continuous data on the sea-level height resulting from surges from which surge probabilities could be estimated. Tide-height distributions were also generated spatially by predicting tides using spatial information on the major tide constituents. These were combined with the storm surges using a JPM and return levels estimated.

Storm surges were found to be largest on the southeast coast of Tasmania and smallest on the northern Tasmanian coast. Storm tides, the combination of surges and tides, on the other hand were largest on the north Tasmanian coast owing to the large tidal range. The effect on storm surges of wind speed changes simulated by one of the Climate Futures for Tasmania model simulations (GFDLCM 2.0) was investigated by adjusting the winds in each event by the wind changes in the 2080-2099 climate relative to the 1980-1999 climate. The changes were found to vary from little change to minor reduction in storm tide height around the Tasmanian coast. Further investigation is warranted to understand the role of wind changes along the southern Australian coast on the Tasmanian coast results presented here but is beyond the scope of the current project. Projected sea-level rise by 2030 will mean that a one-in-100 year event based on late 20th century conditions will occur at least as frequently as a once every 50 years and may occur as frequently as once every 10 years if sea-level rise follows the upper end of the IPCC (2007) projected range. By 2090, the impact of the IPCC (2007) projected range of sea-level rise will mean that a one-in-100 year event based on late 20th century conditions will occur as frequently as once every two to six years depending on location for the low end value of sea-level rise and will occur more than once per year if the high end sea-level rise projections eventuate.

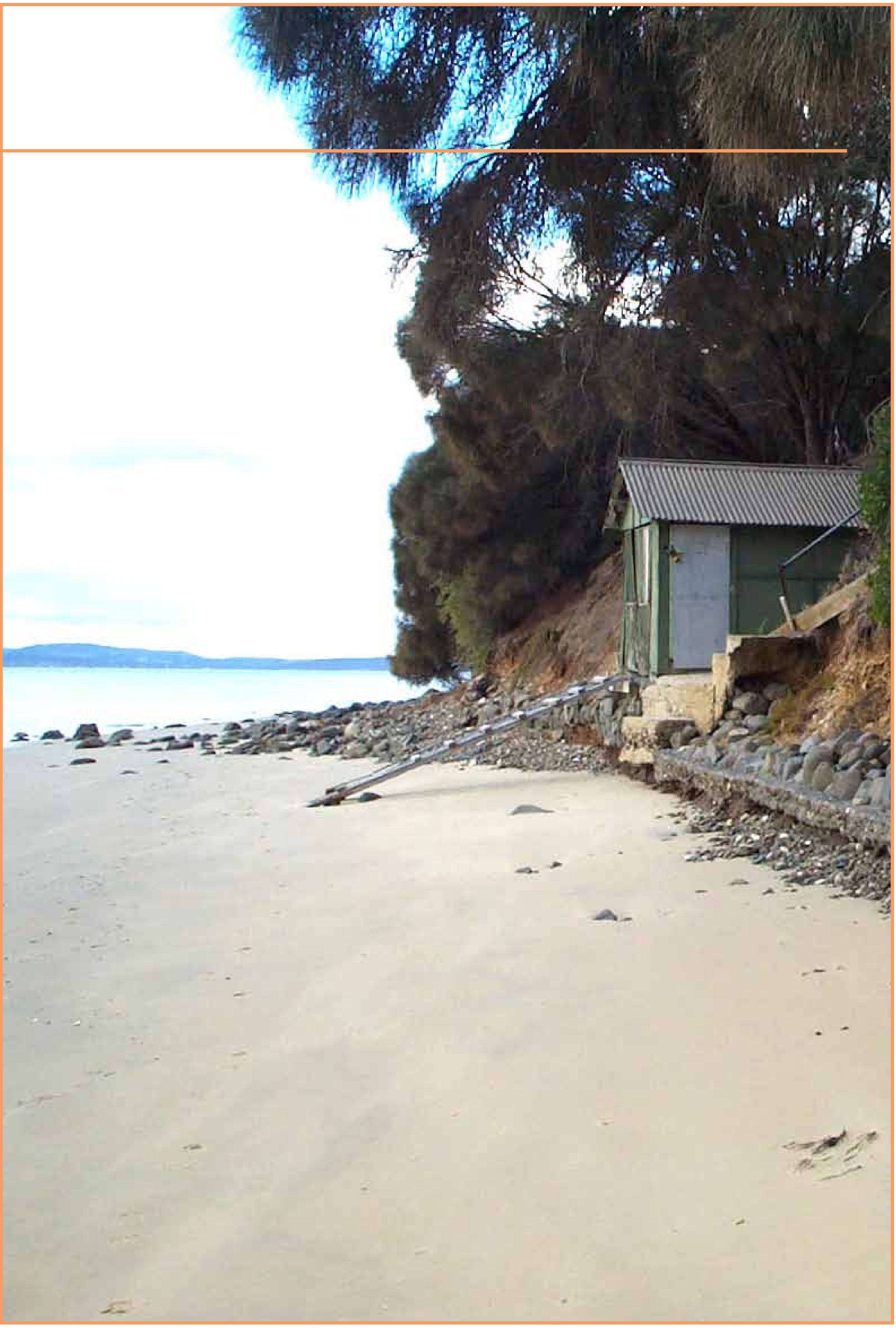

References

Bernier NB & Thompson KR 2006, 'Predicting the frequency of storm surges and extreme sea levels in the northwest Atlantic', *Journal of Geophysical Research*, 111, C10009, DOI 10.1029/2005JC003168.

Bindoff NL, Willebrand J, Artale V, Cazenave A, Gregory J, Gulev S, Hanawa K, Le Quere C, Levitus S, Nojiri Y, Shum CK, Talley LD & Unnikrishnan A 2007, 'Observations: Oceanic Climate Change and Sea Level'. Climate Change 2007: *The Physical Science Basis. Contribution of Working Group I to the Fourth Assessment Report of the Intergovernmental Panel on Climate Change*, [Solomon S, Qin D, Manning M, Chen Z, Marquis M, Averyt KB, Tignor M and Miller HL (eds)]. Cambridge University Press, Cambridge, United Kingdom and New York, NY, USA.

Bureau of Meteorology 2011, http://www.bom.gov.au/oceanography/projects/abslmp/data/index.shtml.

CGIAR-CSI 2008, http://srtm.csi.cgiar.org/index.asp.

Church JA & White NJ 2006, 'A 20th century acceleration in global sea-level rise', Geophysical Research Letters, 33, L01602, DOI 10.1029/2005GL024826.

Church JA, Hunter JR, McInnes KL & White NJ 2006, 'Sea-level rise around the Australian coastline and the changing frequency of extreme sea-level events', *Australian Meteorological Magazine,* vol. 55, pp. 253-260.

Coles SG 2001, *An Introduction to Statistical Modeling of Extreme Values*, Springer, London, UK.

Commonwealth of Australia 2007, *Australian Tide Tables 2007*, Australian Hydrographic Publication, 368pp.

Corney SP, Katzfey JF, McGregor JL, Grose MR, Bennett JC, White CJ, Holz GK, Gaynor SM & Bindoff NL 2010, *Climate Futures for Tasmania: modelling technical report*, Antarctic Climate & Ecosystems Cooperative Research Centre, Hobart.

Department of Climate Change and Energy Efficiency 2009, *Climate Change Risks to Australia's Coast. A First Pass National Assessment*. Australian Government Department of Climate Change, 172pp, http://www.climatechange.gov.au/~/media/publications/coastline/cc-risks-full-report.ashx

Foreman GG 1977, *Manual for Tidal Heights Analysis and Prediction*, Pacific Marine Science Report 77-10, Institute of Ocean Sciences, Victoria, Canada, 98pp.

Geoscience Australia 2008, https://www.ga.gov.au/products/servlet/controller?event=GEOCAT_DETAILS&catno=66006.

Godin G 1972, *The Analysis of Tides*, University of Toronto Press, Toronto, Canada.

Hemer M, McInnes KL & Ranasinghe R 2010, *Investigation of climate change driven variations in offshore wave climate along the NSW coast.* Final Report for Department of Climate Change and Energy Efficiency, 64pp.

Horsburgh KJ, Wilson C 2007, 'Tide-surge interaction and its role in the distribution of surge residuals in the North Sea', *Journal of Geophysical Research*, 112, C08003.

Hubbert GD & McInnes KL 1999, 'A storm surge inundation model for coastal planning and impact studies', *Journal of Coastal Research*, vol. 15, 168-185pp.

Hunter J, 2010, 'Estimating sea-level extremes under conditions of uncertain sea-level rise', *Climatic Change* 93: 331-350, DOI 10.1007/s10584-009-9671-6.

Jansen E, Overpeck J, Briffa KR, Duplessy J-C, Joos F, Masson-Delmotte V, Olago D, Otto-Bliesner B, Peltier WR, Rahmstorf S, Ramesh R, Raynaud D, Rind D, Solomina O, Villalba R & Zhang D 2007, 'Palaeoclimate'. *Climate Change 2007: The Physical Science Basis. Contribution of Working Group I to the Fourth Assessment Report of the Intergovernmental Panel on Climate Change* [Solomon S, Qin D, Manning M, Chen Z, Marquis M, Averyt KB, Tignor M, Miller HL (eds)]. Cambridge University Press: Cambridge, United Kingdom and New York, NY, USA.

Kalnay EM, Kanamitsu R, Kistler W, Collins DR, Deaven L, Gandin M, Iredell S, Saha G, White J, Woollen Y, Zhu A, Leetmaa B, Reynolds M, Chelliah W, Ebisuzaki W, Higgins J, Janowiak KC, Mo C, Ropelewski J, Wang R, Jenne & Joseph D 1996, 'The NCEP/NCAR 40-Year Reanalysis Project', *Bulletin American Meteorological Society,* vol. 77, pp. 437–471.

Kirchhofer W 1973, *Classification of European 500-mb patterns*, Arbeitsbericht der Schweizerischen Meteorologischen Zentralanstalt Nr. 43, Geneva.

McGregor JL & Dix MR 2008, *An updated description of the conformal-cubic atmospheric model,* High Resolution Simulation of the Atmosphere and Ocean, Hamilton K and Ohfuchi W (eds), Springer, pp. 51-76.

McInnes KL & Hubbert GD 2003, 'A numerical modeling study of storm surges in Bass Strait', *Australian Meteorological Magazine*. vol. 52, pp 143-156.

McInnes KL, Abbs DJ & Bathols JA 2005, 'Climate Change in Eastern Victoria', *Stage 1 Report: The effect of climate change on coastal wind and weather patterns.* Report to Gippsland Coastal Board, 26pp.

McInnes KL, Macadam I, Abbs D & O'Grady J 2009a, *The Effect of Climate Change on Extreme Sea Levels in the Tamar River Estuary,* Report for the Launceston City Council by the Antarctic Climate & Ecosystems Cooperative Research Centre, 30pp.

McInnes KL, Macadam I & O'Grady J 2009b, *The Effect of Climate Change on Extreme Sea Levels along Victoria's Coast*, Report for Victorian Department of Sustainability and Environment, 58 pp.

McInnes KL, Macadam I, Hubbert GD & O'Grady JG. 2009c, 'A Modelling Approach for Estimating the Frequency of Sea Level Extremes and the Impact of Climate Change in Southeast Australia', *Natural Hazards* 51 115–137. DOI 10.1007/s11069-009-9383-2.

Menendez M & Woodworth PL 2010, Changes in extreme high water levels based on a quasi-global tide-gauge data set, *Journal of Geophysical Research*, 115, C10011.

Mount R, Lacey M & Hunter J 2010, *Tasmanian Coastal Inundation Mapping Project,* Report for Tasmanian Planning Commission.

Nakićenović N & Swart R (eds), 2000, Special Report on Emissions Scenarios, a Special Report of Working Group III of the Intergovernmental Panel on Climate Change, Cambridge University Press, Cambridge, UK, and New York, USA, 599pp.

Pugh DT & Vassie JM 1980, 'Applications of the joint probability method for extreme sea level computations', *Proceedings of the Institute of Civil Engineering*, Part 2, 69, 959-975.

Rahmstorf S, 2007. A semi-empirical approach to projecting future sea-level rise. *Science* 315(5810): 368-370.

Sharples C 2006, *Indicative Mapping of Tasmanian Coastal Vulnerability to Climate Change and Sea-Level Rise: Explanatory Report (Second Edition)*, Consultant Report to Department of Primary Industries & Water, Tasmania, 173 pp., plus accompanying electronic (GIS) maps.

Tawn JA & Vassie JM 1989, Extreme sea levels: the joint probabilities method revisited and revised, *Proceedings of the Institute of Civil Engineering*, Part 2, 87, 429-442.

Taylor K 2000, *Summarising multiple aspects of model performance in a single diagram*, PCMDI Report No. 55, 29pp.

Taylor KE 2001, 'Summarizing multiple aspects of model performance in single diagram', *Journal of Geophysical Research,* 106, D7, 7183--7192.

Uppala SM, Kallberg PW, Simmons AJ, Andrae U, Da Costa Bechtold V, Fiorino M, Gibson JK, Haseler J, Hernandez A, Kelly GA, Li X, Onogi K, Saarinen S, Sokka N, Allan RP, Andersson E, Arpe K, Balmaseda MA, Beljaars ACM, Van de Berg L, Bidlot J, Bormann N, Caires S, Chevallier F, Dethof A, Dragosavac M, Fisher M, Fuentes M, Hagemann S, Hólm E, Hoskins BJ, Isaksen L, Janssen PAEM, Jenne R, McNally AP, Mahfouf J-F, Morcrette J-J, Rayner NA, Saunders RW, Simon P, Sterl A, Trenberth KE, Untch A, Vasiljevic D, Viterbo P & Woollen J 2005, 'The ERA-40 re-analysis', *Quarterly Journal of the Royal Meteorological Society,* 131: 2961–3012.

Yarnal B 1993, *Synoptic Climatology in Environmental Analysis,* Belhaven Press: London.

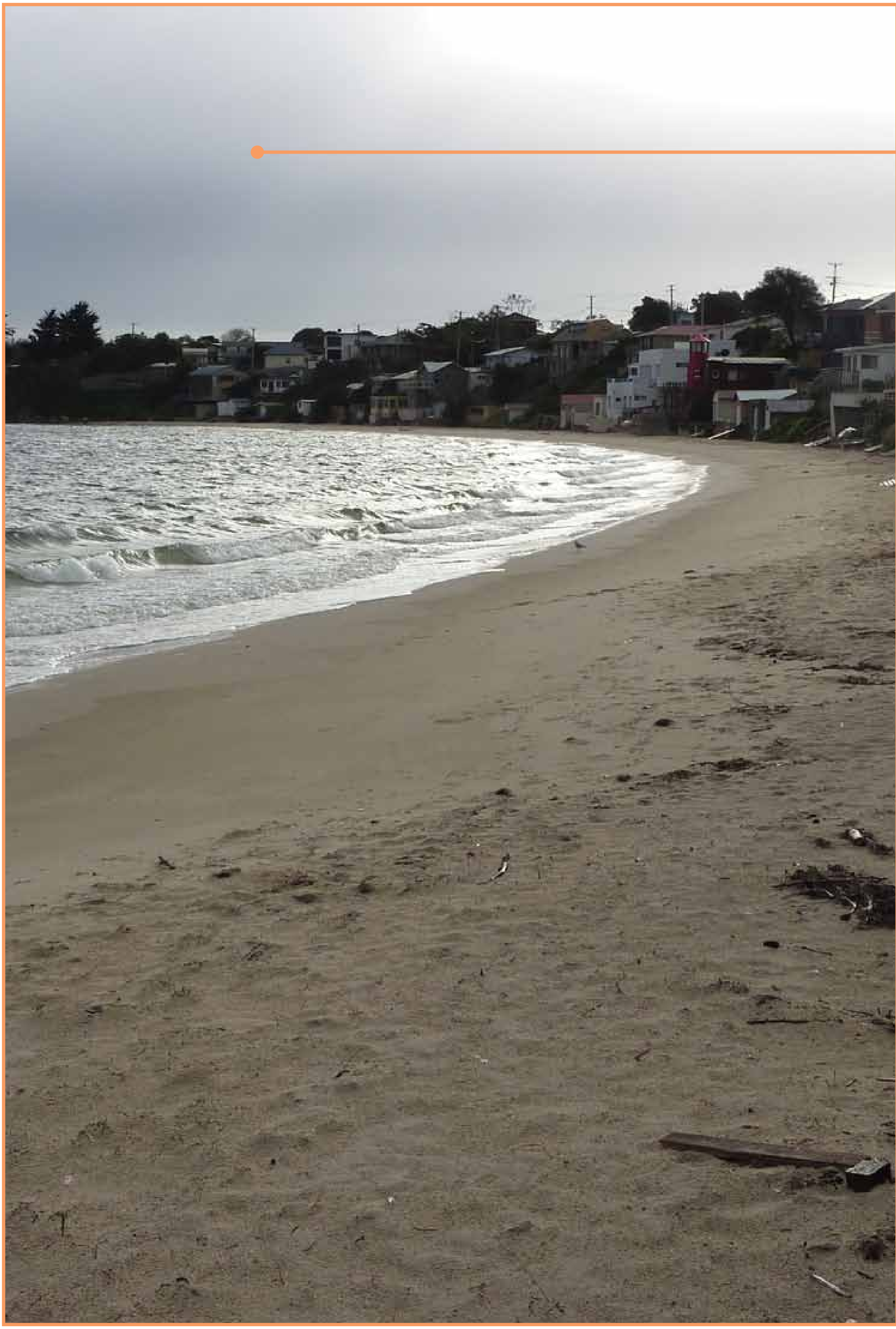

Project Acknowledgements

The Climate Futures for Tasmania project was funded primarily by the State Government of Tasmania, the Australian Government's Commonwealth Environment Research Facilities Program and Natural Disaster Mitigation Program. The project also received additional funding support from Hydro Tasmania.

Scientific leadership and contributions were made from a consortium of organisations including: Antarctic Climate & Ecosystems Cooperative Research Centre, Tasmanian Department of Primary Industries, Parks, Water and Environment, Tasmanian State Emergency Service, Entura, Geoscience Australia, Bureau of Meteorology, CSIRO, Tasmanian Partnership for Advanced Computing, Tasmanian Institute of Agricultural Research and the University of Tasmania.

The generation of the Climate Futures for Tasmania climate simulations was commissioned by the Antarctic Climate & Ecosystems Cooperative Research Centre (ACE CRC), as part of its Climate Futures for Tasmania project. The climate simulations are freely available through the Tasmanian Partnership for Advanced Computing digital library at www.tpac.org.au.

Climate Futures for Tasmania is possible with support through funding and research of a consortium of state and national partners.

Climate Futures for Tasmania is possible with support through funding and research of a consortium of state and national partners.

ANTARCTIC CLIMATE & ECOSYSTEMS CRC

Australian Government
Department of Sustainability, Environment, Water, Population and Communities

Tasmania
Explore the possibilities

Australian Government
Attorney-General's Department

State Emergency Service Tasmania

Australian Government
Bureau of Meteorology

Hydro Tasmania
The power of natural thinking

Australian Government
Geoscience Australia

CSIRO

UTAS

tiar
TASMANIAN INSTITUTE OF AGRICULTURAL RESEARCH

TPAC